The Effect of Jaw Clenching on Extracranial and Intracranial Blood Flow

by

Eudoxia Zafiris

A thesis
presented to the University of Waterloo
in fulfillment of the
thesis requirement for the degree of
Master of Science
in
Kinesiology

Waterloo, Ontario, Canada, 2025

© Eudoxia Zafiris 2025

Author's Declaration

I hereby declare that I am the sole author of this thesis. This is a true copy of the thesis, including any required final revisions, as accepted by my examiners.

I understand that my thesis may be made electronically available to the public.

Abstract

The internal carotid artery (ICA) and external carotid artery (ECA) facilitate perfusion to the intracranial and extracranial regions, respectively. Under current dogma, the ICA is tightly regulated to ensure stable cerebral perfusion, while the ECA remains more pressure-passive, compensating for fluctuations in blood flow to the brain by redirecting blood flow to protect the cerebrovascular network during physiological stressors. While previous research has attempted to influence ECA flow through indirect stimuli such as facial cooling and exercise, direct experimental manipulation of ECA flow has rarely been tested. It remains unclear how ICA and ECA branches reallocate flow in response to changing demands in the facial vasculature. The purpose of this research is to determine whether the ECA can directly control carotid flow redistribution via jaw clenching by increased facial flow resistance and a post-exercise hyperemic response. 26 healthy adults (24±4 years; 15 female) performed isometric (25% maximum voluntary jaw clench (MVJC); 60 sec) and dynamic (50% duty cycle 3 seconds ON/OFF, for 60 sec at 75% MVJC) jaw clenching exercises. Additionally, a facial cooling mask was placed on each participants face to elicit a non-metabolic vasoconstrictor response. Blood velocity in the CCA, ECA and ICA was measured with conventional Doppler ultrasound before, during, and post clenching periods, and before and during facial cooling. Transcranial Doppler ultrasound continuously recorded middle cerebral artery velocity (MCAv), and vector flow imaging (VFI) was used to scan the carotid bifurcation before and post jaw clenching to determine changes in blood flow patterns. During both isometric and dynamic jaw clenching protocols, CCA and ECA blood flow increased from baseline, during, and post clenching, accompanied by a decrease in the pulsatility index (PI) ($p < 0.05$), indicating that jaw clenching actively increases extracranial blood flow via the ECA. In contrast, no changes were observed in ICA blood flow and PI throughout isometric jaw clenching, however, during dynamic jaw clenching, blood flow increased during the post clench phase compared to the ON phase ($p <$

0.05) and the PI decreased throughout ($p < 0.05$). MCAv increased during dynamic clenching ($p < 0.05$). The resistance index decreased during clenching and rebounded post clench for both jaw clenching conditions ($p < 0.05$), suggesting that intracranial responses depend on the clenching modality. VFI revealed that isometric jaw clenching increased flow and uniformity at the carotid bifurcation, reflecting laminar redistribution between the ECA and ICA. These findings provide novel evidence that jaw clenching can modulate carotid hemodynamics at both extracranial and intracranial levels and reshape local flow patterns at the carotid bifurcation. This has potential implications for understanding vascular contributions to temporomandibular disorders and the broader cerebrovascular impact of chronic jaw muscle activity.

Acknowledgements

What a journey! This has been such a fulfilling experience, one that has allowed me to grow as an individual and has given me the confidence to truly believe in what I am capable of.

Thank you, Dr. Jason Au, for giving me this opportunity and believing in me. Your guidance and support have been invaluable, and I am especially grateful for the freedom you gave me to think outside the box and share my passion for the dental field in a unique way. Coming into this without a kinesiology background and no prior research experience was daunting, but you saw my potential and trusted in my work ethic. As a student, it means so much to have someone recognize and invest in what I can do.

To my committee members, Dr. Andrew Robertson and Dr. Michaela Devries-Aboud, thank you for joining me on this journey and for helping bring everything together.

To my parents, thank you for being my unwavering support system. In moments of doubt or when I felt like giving up, you reminded me how far I've come and encouraged me to keep reaching for my goals and passions.

To my lab mates and friends, thank you for all the giggles, coffees, snacks, and little boosts along the way.

And lastly, but most importantly, I thank God for giving me the strength to move past doubts and insecurities, to fully trust the process, and to embrace each step of this journey.

Table of Contents

List of Figures ..... *viii*

List of Tables ..... *ix*

List of equations ..... *x*

List of Acronyms ..... *xi*

1.0 Literature review *1*

1.1 Major extracranial arteries **4**

1.1.1 Common carotid artery and blood flow patterns 4

1.1.2 Internal carotid artery anatomy and blood flow 6

1.1.3 External carotid artery anatomy and blood flow 8

1.1.4 Carotid bifurcation disturbed blood flow patterns 10

1.2 Major Intracranial Arteries **13**

1.2.1 Cerebrovascular Blood Flow and Autoregulation 13

1.2.2 Importance of the facial arterial network 16

1.3 Current ultrasound methods to measure complex blood flow **18**

2.0 Study rationale *21*

3.0 Research Questions and Hypotheses *22*

4.0 Methods *23*

4.1 Ethics **23**

4.2 Participants **23**

4.3 Sample size calculation **24**

4.4 Study Design **26**

4.5 Experimental measures **29**

4.5.1 Data Acquisition 29

4.5.2 Data Processing 33

4.6 Statistical analysis **39**

5.0 Results *42*

5.1 Participant Characteristics **42**

5.2 Carotid artery blood flow **43**

5.3 Middle Cerebral Artery Velocity **47**

5.4 Vector Flow Imaging **48**

5.5 Electromyography **50**

6.0 Discussion *53*

6.1 Extracranial Blood Flow Response **53**

6.2 Intracranial Blood Flow and Cerebrovascular Response **55**

6.3 Blood Flow Redistribution **58**

6.4 Blood Flow Patterns **61**

6.5 Facial Cooling **62**

6.6 Clinical Significance in Dentistry **63**

7.0 Limitations *66*
8.0 Conclusion *68*
References *69*
Appendix A: Figure Permissions *84*

List of Figures

Figure 1: Vector flow image of a carotid bifurcation depicting flow reversal at the carotid bulb 2
Figure 2: Anatomical Variations of the carotid bifurcation and its branches 5
Figure 3: Visual representation of angle and radius measurements taken from the carotid artery at the bifurcation 6
Figure 4: Vector flow images illustrating disturbed flow patterns in stenosed ICAs 8
Figure 5: Circulatory pathways of the external carotid artery and its collateral vascular connections with the internal carotid system 9
Figure 6: Carotid artery with atherosclerosis 11
Figure 7: Cerebral autoregulation 14
Figure 8: Vector flow image scan of the carotid bifurcation in a 23-yr-old male 19
Figure 9: G*Power analysis output 25
Figure 10: Timeline of study protocol 28
Figure 11: Participant experimental setup 28
Figure 12: Raw mean blood velocity tracings 35
Figure 13: Raw tracing of right middle cerebral artery velocity and right masseter electromyography from a 24-yr-old male 37
Figure 14: Blood flow throughout the protocol 45
Figure 15: Pulsatility index throughout the protocol 46
Figure 16: Percent blood flow distribution metrics 47
Figure 17: Middle cerebral artery velocity and resistance index 48
Figure 18: Representative qualitative vector flow images of the carotid bifurcation in a 27-yr-old male 49
Figure 19: Statistical analysis of vector flow imaging results 50

List of Tables

Table 1: Participant characteristics 42
Table 2: Temperatures recorded during facial cooling mask protocol. 43
Table 3: Percent blood flow redistribution metrics 51
Table 4: Cardiovascular, cerebral, and muscle activation responses across experimental conditions. 51

List of equations

Equation 1: Blood flow 34
Equation 2: Pulsatility index 35
Equation 3: Resistance index..... 36
Equation 4: Fatigue index..... 38

List of Acronyms

CA: cerebral autoregulation

CBF: cerebral blood flow

CCA: common carotid artery

CO: cardiac output

CO_2: carbon dioxide

ECA: external carotid artery

EMG: electromyography

FI: fatigue index

GCA: giant cell arteritis

ICA: internal carotid artery

LDL: low-density lipoprotein

MCA: middle cerebral artery

MCAv: middle cerebral artery velocity

MVJC: maximum voluntary jaw clenching force

N: Newtons

PI: pulsatility index

Re: Reynold's number

RI: resistance index

RMS: root mean square

TCD: transcranial Doppler ultrasound

TMD: temporomandibular disorder

VCC: vector concentration coefficient

VFI: vector flow imaging

WSS: wall shear stress

1.0 Literature review

The common carotid arteries (CCA), located on both sides of the neck, are the primary blood vessels for supplying blood to the neck, head, and facial region (1). As the CCA ascends the neck, it will bifurcate, giving rise to the internal carotid artery (ICA) and external carotid artery (ECA) which are the main branches responsible in facilitating hemodynamic perfusion to the cerebral (intracranial) and facial (extracranial) regions respectively (1). While many carotid arteries follow a relatively straight course, there are variations where some carotid arteries have kinks or curves along their path (Fig. 2) (2). The location of the bifurcation can also vary, with some located lower in the neck, and others higher up (Fig. 2) (2). Interestingly, the carotid bifurcation is a frequent site for atherosclerotic plaque development due to disturbed blood flow patterns that arise from these anatomical and geometric variabilities mentioned (3). Typically, blood flows in layers that move parallel to one another along the length of the vessel, a phenomenon known as laminar flow. In this arrangement, faster-moving blood is concentrated in the center of the vessel, while slower-moving blood is found near the vessel walls due to the effects of friction (4). Regions such as the carotid bifurcation, do not exhibit laminar flow; instead, disturbed flow patterns arise which are characterized by flow separation, recirculation zones, and flow reversal (3,4). Disturbed flow leads to endothelial dysfunction, a key factor contributing to the development of atherosclerosis (5). In particular, located near the carotid bifurcation and in close proximity of the ICA, the carotid sinus is a region where blood flow encounters a boundary layer separation zone where flow patterns may briefly reverse direction resulting in transient blood flow reversal (Fig. 1) (6,7). These localized flow disturbances may influence upstream regulatory mechanisms responsible for maintaining cerebral perfusion.

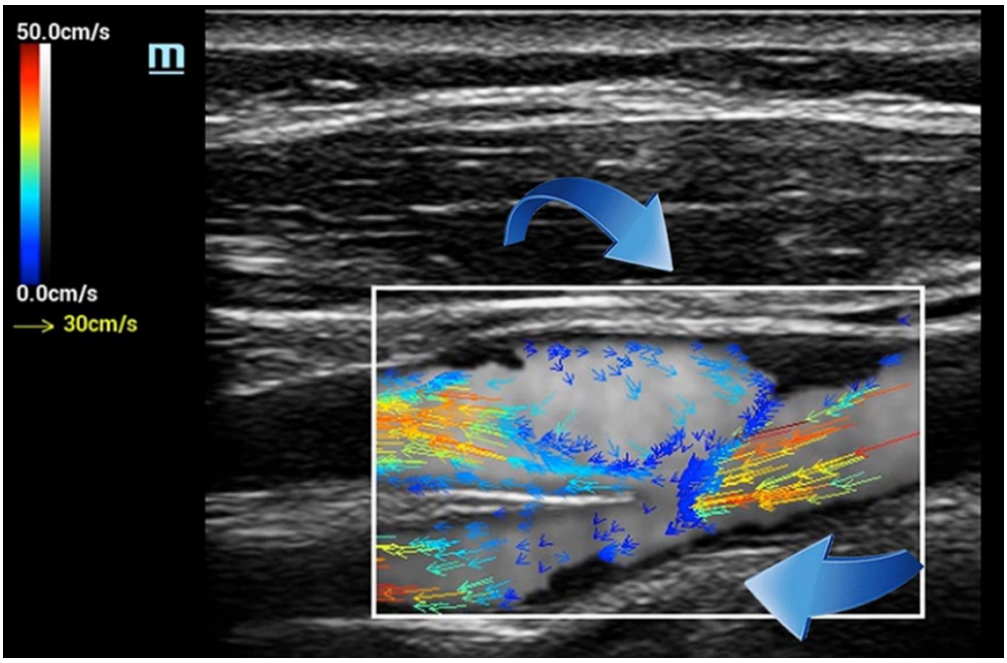


Figure 1: Vector flow image of a carotid bifurcation depicting flow reversal at the carotid bulb. Lower velocity is represented by blue vector arrows pointed towards the right. Retrieved from Baun (7).

Given the brain's exceptionally high metabolic demand, stable blood flow is essential for maintaining adequate oxygenation and sustaining vital brain function (8). To achieve this, the brain relies on cerebral autoregulation, a tightly controlled process that ensures consistent cerebral blood flow despite fluctuations in mean arterial pressure and perfusion pressure (9). While the ICA is tightly regulated to ensure stable cerebral perfusion, the ECA remains more pressure-passive, compensating for fluctuations in blood flow to the brain by either absorbing or redirecting flow to protect the cerebrovascular network (10–12). The ECA is primarily responsible for supplying blood to the facial region; however, in severe cases where the ICA becomes occluded due to plaque formation, the ECA can facilitate collateral pathways, forming extracranial-to-intracranial connections that help maintain cerebral perfusion (13). Additionally, during physiological stressors, such as intense exercise or facial cooling, the ECA may act as a safeguard against cerebral over- and under-perfusion (14–16). Therefore, this suggests that changes in vascular tone within the downstream branches of the ECA may

influence upstream blood flow dynamics in the ICA, further underscoring the ECA's role in supporting cerebrovascular stability under varying physiological conditions (17).

While the ECA can be considered pressure-passive and serve as a protective mechanism to ensure proper recovery of ICA blood flow and optimize intracranial oxygen delivery; it remains unclear whether the ECA can directly regulate flow redistribution at the carotids, particularly in response to experimental manipulation of resistance in the downstream facial arterial network. This review will examine the anatomy and blood flow patterns of major extra- and intra-cranial arteries and probe the utility of the ECA as a target artery for extracranial blood flow control. Additionally, this review will examine the flow distribution between the ICA and ECA, specifically examining the blood flow dynamics at the carotid bifurcation. The flow distribution between the ICA and ECA serves as a good model for extracranial flow control since it highlights the balance between tightly regulated intracranial flow (ICA) and more pressure-passive flow to the face (ECA). This balance offers valuable insights into how blood flow can be manipulated to meet local demands, and how disturbances in flow might lead to vascular dysfunction. Jaw clenching will be used as a stimulus to induce increased peripheral resistance and a post-exercise hyperemic response, while facial cooling will be used to constrict facial arteries and elicit a non-metabolic vasoconstrictor response.

1.1 Major extracranial arteries

1.1.1 Common carotid artery and blood flow patterns

The CCAs run bilaterally along the neck and are the primary blood vessels responsible for facilitating hemodynamic perfusion to the cerebral and facial regions (1). The CCA originates posterior to the sternoclavicular joints in the neck and is contained within the carotid sheath posterior to the sternocleidomastoid muscle (18). Originating differently on each side, the right CCA stems from the brachiocephalic artery, while the left CCA arises directly from the aortic arch in the thorax (19). The arterial vasculature is composed of three tissue layers: the tunicas intima, media, and adventitia (20). The tunica intima is the innermost layer of the arterial wall, consisting of a single layer of endothelial cells that line the lumen, serving as a conduit for blood to flow through the lumen (21). The tunica media, the middle arterial layer composed of smooth muscle cells, elastin, and collagen, is responsible for mechanical properties by passively distending and recoiling in response to changes in blood pressure (4). The tunica adventitia is the outermost layer which connects the carotid vessel to the surrounding tissue, serving as an anchor to ensure proper attachment and support (21).

As the CCA ascends the neck, it reaches the carotid bifurcation where it divides into two daughter branches of unequal size, giving rise to the ICA and ECA (22,23). There is considerable variability in height, location, and geometric configuration of the bifurcation across individuals that strongly influences hemodynamic patterns within the vasculature (2,24). Studies indicate that approximately 63% of CCAs follow a straight course, while 26% exhibit curvature, and 6% display kinking or coiling, indicative of varying degrees of tortuosity within the CCA architecture (Fig. 2) (2,25). These anatomical and geometric variabilities in the carotid bifurcation may contribute to an increased likelihood of turbulent flow (26). Turbulent flow consisting of chaotic and randomized flow in all directions can arise in the posterolateral aspect

of the carotid sinus and is often associated with conditions such as atherosclerosis and stenosis (6,26). This irregularity in blood flow causes pressure and velocity to fluctuate within the vessel resulting in endothelial damage and plaque formation which in turn reduces the efficiency of blood flow and nutrient delivery to tissues (27).

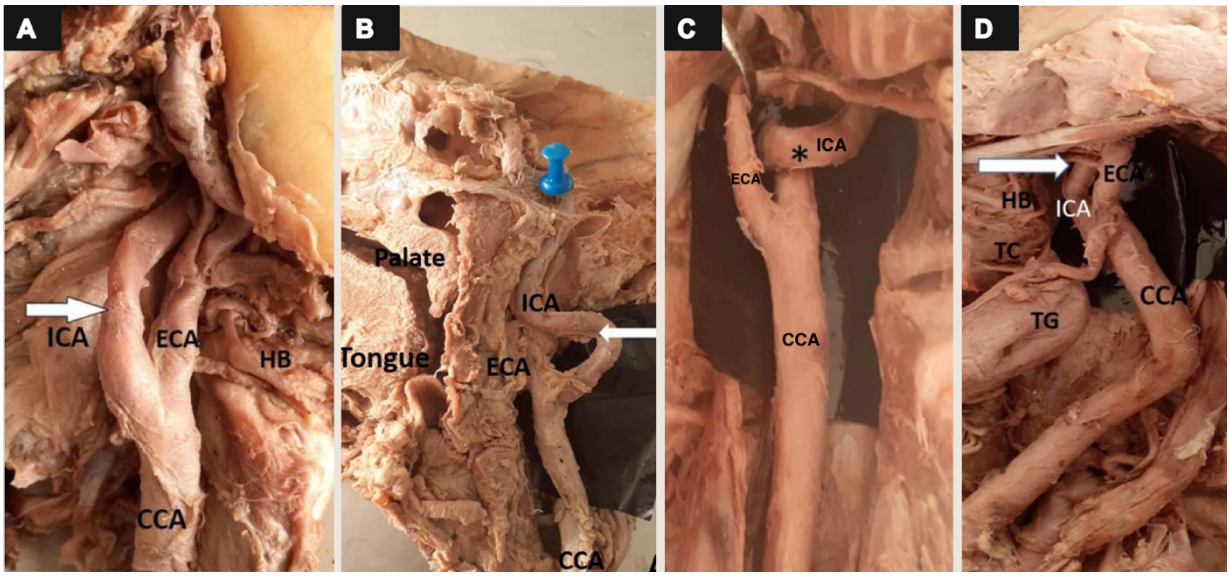


Figure 2: Anatomical Variations of the carotid bifurcation and its branches. The ICA may follow a curved course (A), demonstrate kinking (B), or exhibit coiling (C). Additionally, the carotid bifurcation may vary in its location, appearing higher in the neck above the level of the hyoid. Adapted from Arumugam and Subbiah (25).

To quantify the onset of turbulence and to predict when flow becomes inefficient, Reynold's number (Re) is used in fluid dynamics when transitioning from laminar to turbulent flow (28). When Re exceeds a certain threshold (typically greater than 4000), the flow shifts from laminar to turbulent, amplifying the irregularities in velocity and pressure within the vessel, and thereby decreasing flow efficiency (29).

The hemodynamic environment of the carotid artery is characterized by a diverse range of blood flow patterns. Investigating the CCA, this section exhibits plug flow, a distinct type of laminar flow characterized by a flattened blood flow profile in the middle of the vessel, where blood moves at a relatively uniform speed (30). As we ascend the CCA, blood flow remains laminar, however, reaching the carotid bifurcation, this is where flow patterns become disturbed exhibiting patterns such as flow separation, turbulence and recirculation (31).

Interestingly, anatomical differences can markedly influence the formation of recirculation zones and turbulent flow, which may increase the risk of vascular complications such as atherosclerosis. Recirculation is characterized by streamlines looping from the forward flow into a zone where the flow has separated from the vessel wall (31). Notably, there is a correlation between bifurcation angle (Fig.3) and sex, revealing that males typically exhibit larger bifurcation angles than females (32). The average bifurcation angle for females is approximately 51 degrees, while for males, it averages around 67 degrees (33). Specifically, a larger ICA angle (>25°) has been associated with abnormal wall shear stress (WSS) patterns, including the formation of recirculation zones and low WSS which can contribute to atherosclerotic plaque development (34,35).

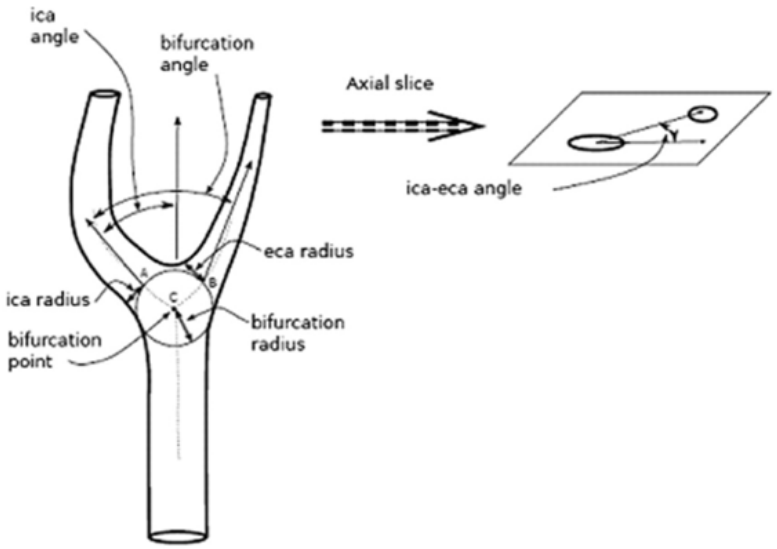


Figure 3: Visual representation of angle and radius measurements taken from the carotid artery at the bifurcation. Adapted from Phan et al (34).

1.1.2 Internal carotid artery anatomy and blood flow

The ICAs are responsible for delivering oxygenated blood to the brain and are divided into extracranial and intracranial parts, with several distinct segments (36,37). The ICA begins as one of the terminal branches of the CCA at the carotid bifurcation, enters through the base of the skull, and travels upwards through the outer opening of the carotid canal in the petrous

temporal bone (36,37). The ICA passes through the foramen lacerum, the cavernous sinus, and enters the subarachnoid space (36). Within the cranial cavity, the ICAs anastomose with the vertebral arteries to form the circle of Willis, supplying the brain with blood (38). The final segment of the ICA branches into the ophthalmic, middle cerebral, and anterior cerebral arteries (38).

When using Doppler ultrasonography to assess blood velocity in the ICA, the waveform appears as a low resistive pattern, and the velocity difference between systolic and diastolic phases are smaller than the ECA (39). This is reflected by a low pulsatility index (PI), defined as the difference between the peak systolic flow and minimum diastolic flow velocity, divided by the mean velocity recorded throughout a cardiac cycle (40). While the PI is often used to assess vascular resistance, its relationship with actual vascular or cerebrovascular resistance is variable and influenced by several factors, including cerebral perfusion pressure, heart rate, and arterial compliance (41,42). Since the ICA is responsible for supplying blood to the brain, it is crucial that blood flow is tightly regulated to ensure optimal cerebral circulation. A reduction in pulsatility along the ICA is thought to help buffer the cerebral microvasculature from excessive pulse pressures (43,44). In this context, a lower PI may reflect more effective dampening of blood flow pulsatility, ensuring protection against potential damage caused by high pulsatility and promoting stable, efficient circulation to the brain (43).

Regarding blood flow dynamics, the ICA exhibits complex hemodynamic flow patterns. At the base of the ICA near the carotid sinus, a recirculation zone is formed (Fig. 4) (45). Transient flow reversal, involving temporary changes in the direction of blood flow, is also observed during systole near the ICA (Fig. 4) (46). Although these flow patterns mentioned are considered common in the ICA, over time, these disturbed flow patterns can contribute to an increased likelihood of plaque development in this region (45–48).

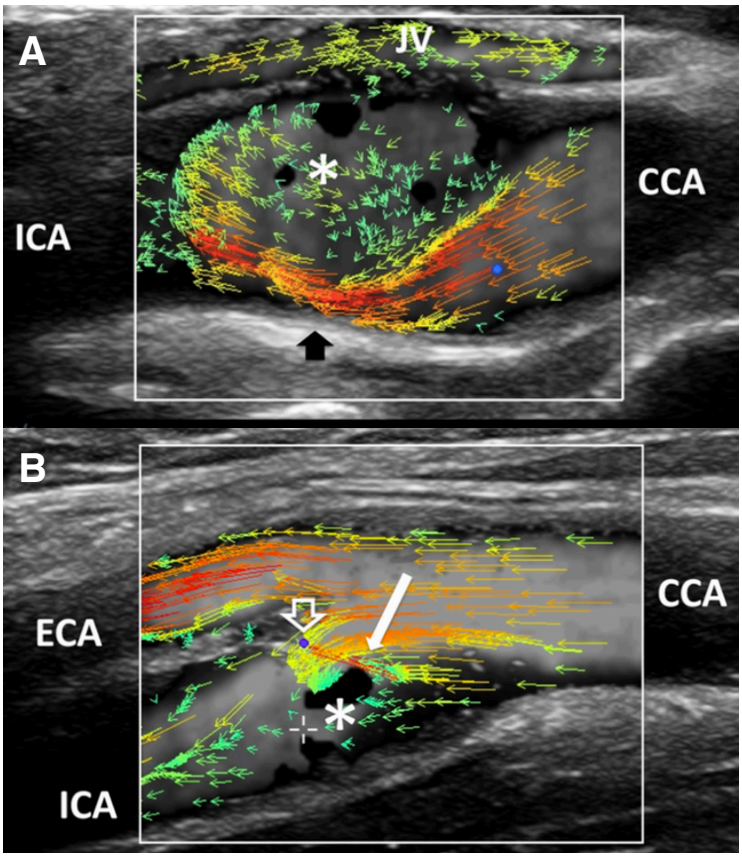


Figure 4: Vector flow images illustrating disturbed flow patterns in stenosed ICAs. (A) Short green vectors (*) highlight a large vortex, indicating flow recirculation within the enlarged ICA bulb in the presence of low-degree stenosis. High-velocity vectors follow the posterior wall (black arrow). (B) In moderate ICA stenosis, flow reversal represented as red vectors (arrow) move retrograde from the flow separation point (blue dot, void arrow). High-velocity forward flow velocities at the stenosis are depicted by orange and yellow vectors. Retrieved from Goddi et al (31).

1.1.3 External carotid artery anatomy and blood flow

The ECA is the second branch that divides from the carotid bifurcation at the level of the superior border of the thyroid cartilage (49). It runs superiorly and posteriorly between the neck of the mandible and the earlobe to supply blood to the neck, face, scalp, skull, and meninges (17,50). The ECA extensively divides into eight main branches: the superior thyroid artery, ascending pharyngeal artery, lingual artery, facial artery, occipital artery, posterior auricular artery, superficial temporal artery, and maxillary artery (51).

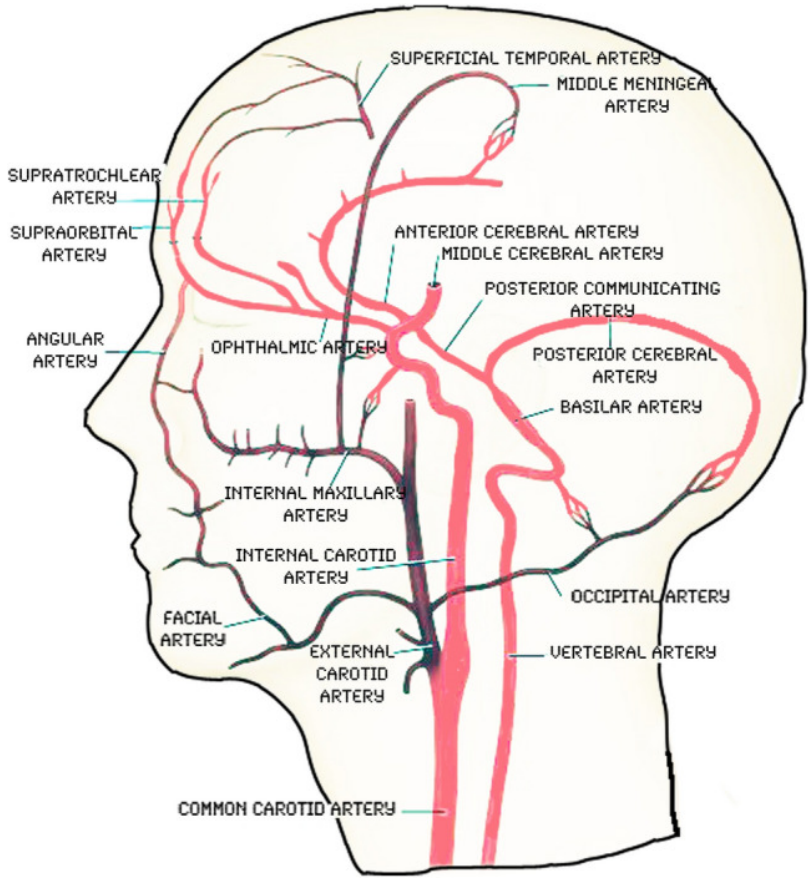


Figure 5: Circulatory pathways of the external carotid artery and its collateral vascular connections with the internal carotid system. Retrieved from Miceli et al (52). (52)

The ECA holds considerable clinical significance regarding surgical procedures since it allows for a bypass between the superficial temporal artery and the middle cerebral artery (MCA) outside the skull, creating an alternate route for blood flow to the brain (53). The most important features are the anastomoses to the ophthalmic artery around the orbit and nose and to the vertebral artery through the superior and inferior thyroid arteries and branches of the occipital artery (53). This creates a collateral pathway, particularly critical in emergencies like ICA occlusion, guaranteeing continuous blood supply to the brain via interconnected vessels in the event of primary artery blockage (53).

When using Doppler ultrasonography to assess blood velocity in the ECA, the Doppler waveform shows a larger difference in the velocity between systolic and diastolic phases compared to the ICA (39). Additionally, the ECA displays high pulsatility flow characteristics

due to the high peripheral resistance of the vascular bed it supplies (54). Flow in the ECA is typically laminar; however, flow reversal between the ECA and the ICA, as well as recirculation zones, can occur due to the flow-dividing structure of the carotid bifurcation (46,55,56). Although the ECA is rarely affected by stenosis (57), inflammation affecting its distal branches can be clinically significant. This is particularly evident in conditions such as giant cell arteritis (GCA), where the smaller branches of the ECA, such as the superficial temporal artery, become prime targets for chronic inflammation (58). GCA is an autoimmune disease characterized by the accumulation of granulomas, clusters of immune cells, within blood vessels resulting in inflammation (59). Chronic inflammation will damage the vascular endothelium producing scar tissue leading to the thickening and narrowing (60). Symptoms of GCA include, temporal headaches, and scalp tenderness, however, a common symptom experienced by many is jaw claudication (61). Jaw claudication is presumably due to inflammation of the ECA branches, the internal maxillary artery, and facial artery, which supply blood to the mandibular muscles, along with the temporal artery (62). As a result, blood flow in these regions are reduced and lead to pain or fatigue in the mandibular muscles, particularly when chewing, and typically resolves when chewing stops (63).

1.1.4 Carotid bifurcation disturbed blood flow patterns

Atherosclerosis is primarily initiated by endothelial injury, which triggers a chronic inflammatory response characterized by the abnormal deposition and hardening of low-density lipoprotein (LDL) cholesterol (64). This endothelial damage leads to the accumulation of plaque within the arterial lumen (Fig. 6). As plaque builds up, it perpetuates a cycle of inflammation that further injures the endothelium (64). As blood flows through a vessel, it exerts a frictional force on the vessel wall known as WSS, a key hemodynamic parameter closely associated with the development of atherosclerotic disease (65,66). Plaque progression

has been strongly linked to areas exhibiting low and/or oscillatory WSS creating conditions conducive to the retention of LDL particles and the infiltration of inflammatory cells (66,67). Low WSS is believed to promote intimal plaque accumulation through two key mechanisms. First, the reduced shear rates can impair the transport of circulating LDL particles away from the vessel wall, leading to increased deposition and retention within the intima (22). Second, low WSS may interfere with the adequate turnover of essential substances at the endothelial surface, disrupting both the nutrition of the arterial wall and the maintenance of optimal endothelial metabolic function (22). This in turn reduces the production of nitric oxide, which normally has an atheroprotective effect on endothelium and promotes oxidative stress and inflammation (68).

High WSS is generally considered to protect against atherogenesis, however, it can influence the progression of existing plaques by promoting structural changes associated with increased vulnerability and a higher risk of rupture (66,69). As plaque accumulates, the vessel narrows, or in some cases if the plaque ruptures, leading to stenosis or complete occlusion. As a result, cerebral blood flow (CBF) becomes impaired, therefore increasing the risk of experiencing an ischemic stroke, with significant risk emerging when stenosis in the ICA reaches approximately 50–69%, particularly in symptomatic patients (70) .

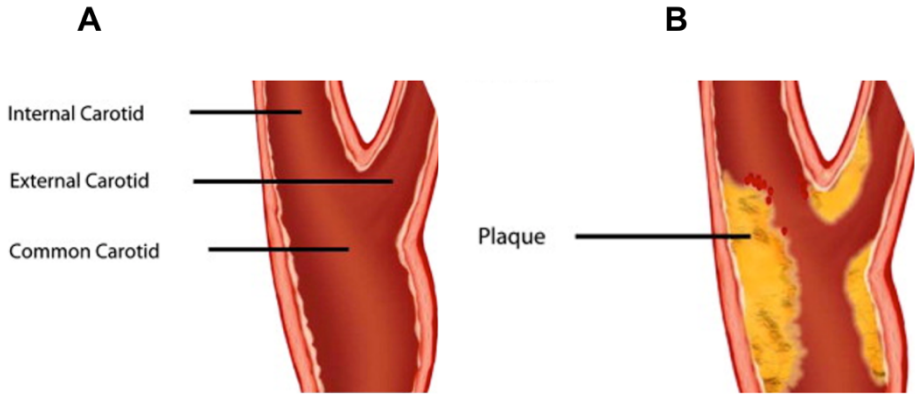


Figure 6: Carotid artery with atherosclerosis. (A) Healthy carotid artery. (B) Carotid artery with accumulation of plaque in the lumen. Adapted from Treat-Jacobson et al (71). (71)

Quantitative analyses reveal intimal thickening is most pronounced within the carotid sinus, opposite to the flow divider (22). This region exhibits flow patterns characterized by separation, vortex formation, decreased velocity, and retrograde flow (22). This environment also produces recirculation zones characterized by low and oscillating WSS (68). In regions with geometrical irregularities, the disturbed and pulsatile flow leads to the development of low WSS conditions (68).

Additionally, distinct anatomical features of the carotid bifurcation can impact plaque formation, such as vessel diameter and area ratios (24). The size of vortices notably increases with an increase in the area ratio, defined as the sum of the cross-sectional areas of the daughter vessels (ICA and ECA) divided by the cross-sectional area of the parent vessel (CCA) (72). Carotid occlusion tends to happen more frequently on the side with the smaller CCA, and smaller CCAs tend to produce more stenotic ICAs. One possible explanation for these findings is that a smaller CCA results in a larger ICA/CCA area ratio (72). Females tend to have larger ICAs compared to males which results in females to have greater outflow to inflow area ratios (73). This ratio compares the combined size of the smaller branches of a blood vessel (ICA and ECA) to the size of the main vessel from which they branch (CCA) (73). It provides a greater understanding of how blood flows through the bifurcation, affecting pulse wave reflection and the stress on vessel walls, which can contribute to plaque formation and vascular damage (73). A larger ratio allows for uniform blood flow and less reflection of the pulse wave whereas, lower ratios can lead to endothelial damage due to increased local stress (73). These differences in anatomy and flow patterns may partly explain the observed variations in plaque distribution and prevalence between sexes.

Additionally, females tend to have smaller carotid arteries compared to males, which could potentially lead to a higher degree of stenosis (74). However, interestingly, males are more prone to developing atherosclerotic plaque formation in the carotid arteries, likely due to

physiological differences in arterial remodeling and the influence of sex hormones (74). Females seem to have superior arterial remodelling abilities, enabling their arteries to adapt more efficiently to blood flow and pressure fluctuations (74). This adaptability may help mitigate the risk of plaque formation, even in the presence of smaller vessel diameters. Additionally, the protective role of estrogen in females may contribute to the lower incidence of carotid plaque formation compared to males (74).

1.2 Major Intracranial Arteries

1.2.1 Cerebrovascular Blood Flow and Autoregulation

Stable blood flow to the brain is essential for maintaining adequate oxygenation and for sustaining vital brain function (9). Without adequate CBF, the brain becomes vulnerable to ischemic damage (9). To meet this demand, the body employs a tightly regulated physiological process known as cerebral autoregulation (CA). CA ensures the ability to regulate CBF via changes in cerebrovascular resistance in response to changes in blood pressure (75,76). CA consists of both static and dynamic components (Fig. 7); however, rather than being distinct physiological entities, these components can be understood as points along a continuum (76). Both static and dynamic autoregulation ensure the brain maintains stable CBF despite changes in blood pressure, however, the difference lies in the time period (76). Static autoregulation measures changes in CBF in response to gradual, sustained shifts in blood pressure, typically over longer periods (10 minutes or more) whereas dynamic autoregulation is measured during rapid changes in blood pressure (seconds to minutes) (75). The mechanisms of CA are not fully understood; however, neurologic, metabolic and myogenic factors contribute to the process (9). Myogenic behaviour of cerebral smooth muscle will either constrict or dilate in response to increases or decreases in cerebral perfusion pressure to protect the brain (77).

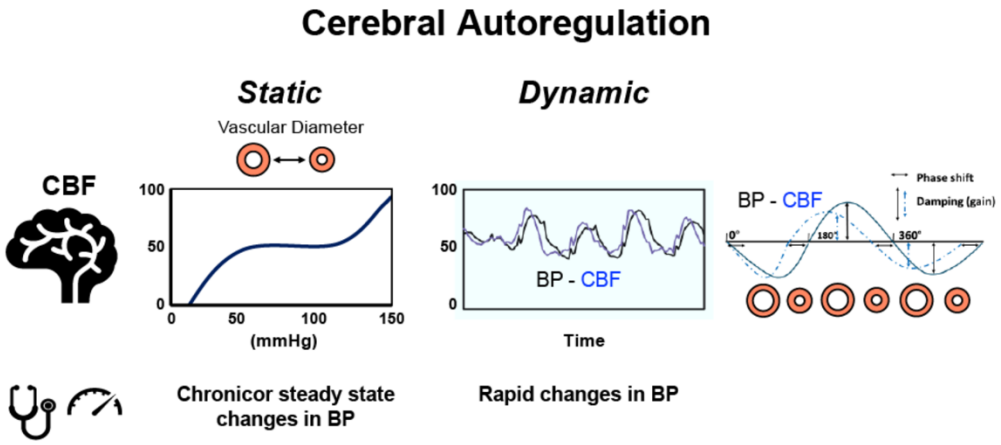


Figure 7: Cerebral autoregulation. Orange circles represent changes in arterial vessel diameter. When changes in blood pressure are minimal, CBF is held stable (static). When blood pressure fluctuates, there is greater variability in CBF (dynamic). Retrieved from Claassen et al (74).

The brain exhibits an exceptionally high metabolic rate, placing a critical demand on blood supply. The brain receives around 15-20% of the body's cardiac output (CO), and changes in CO can impact CBF (78). Although the mechanism is not entirely understood, it is proposed that when CO decreases, the autoregulation curve shows a slight downward shift, reflecting a smaller CBF decrease than the reduction in CO (79). Conversely, an increase in CO leads to a slight upward shift of the autoregulation curve (79). During exercise, CO and mean arterial pressure both increase. Interestingly, vascular resistance in the cerebral circulation appears to rise more significantly than in the peripheral vasculature under these conditions (80). This differential response may represent a protective mechanism mediated by CA, which helps shield the brain from potentially harmful spikes in CO and mean arterial pressure that occur during exercise (80).

Blood to the brain is primarily supplied by the two ICA's and two vertebral arteries, which join to form the circle of Willis (81). This structure provides alternative routes for blood flow in the event of a blockage or narrowing of a vessel (82). It helps to protect the brain against ischemia and allows blood to circulate through interconnected arteries (82). The ICA branches

into the ophthalmic, anterior and middle cerebral artery (MCA); however, the MCA is the largest terminal branch, providing 80% of blood to the cerebral hemispheres (38,83). The MCA is responsible for nourishing the frontal, temporal and parietal lobes of the brain and deeper structures, including the caudate, internal capsule and the basal ganglia (84). These regions contribute to the primary motor and somatosensory cortical areas of the face, trunk, and upper limbs, as well as speech production and comprehension, and writing (84).

CBF is often estimated by measuring mean blood velocity in the MCA (MCAv) using transcranial Doppler ultrasound (TCD) (85,86). TCD cannot directly measure blood flow volume since it does not provide MCA vessel diameter, therefore, it must be assumed that the MCA diameter is not changing (85,86). Fluctuations in arterial carbon dioxide (CO_2) can impact MCA diameter (87,88), and changes in velocity should be interpreted with caution when CO_2 levels aren't stable (89). To account for this, capnography can be used to monitor the partial pressure of CO_2 in exhaled gases, allowing for the detection of subtle breathing pattern changes that may influence arterial CO_2 levels (90).

Through a precise intervention, it may be possible to redirect a fraction of ICA blood flow into the ECA (15). By creating a controlled method to achieve this flow diversion, we can explore how such alterations might impact cerebral perfusion to critical brain regions. For instance, during intense jaw clenching, the masticatory muscles, which are supplied by branches of the ECA, experience increased localized metabolic demands and require enhanced blood flow. If a portion of ICA blood is redirected to the ECA to accommodate this localized demand, it could potentially alter the perfusion of certain brain areas. This scenario allows for the investigation of how changes in blood flow distribution could affect cerebral perfusion, shedding light on vascular adaptations that may occur in response to muscular stress. Although severe jaw clenching is unlikely to produce systemic changes in CBF, it may still serve as a

useful model for examining localized cerebrovascular responses, particularly under conditions of acute mechanical stress.

1.2.2 Importance of the facial arterial network

ECA blood flow regulation and selective redistribution can influence intracranial cerebral hemodynamics. This redistribution mimics the physiological response observed in certain thermoregulatory mechanisms, where a greater portion of blood is diverted through the ECA to regulate temperature (15). Thermoregulation is governed by the body's ability to alter skin blood flow, either by vasodilation to dissipate heat or by vasoconstriction to minimize heat loss (91). The ECA helps manage changes in CBF and safeguards against over- and under-perfusion (14). During dynamic heavy exercise, a reciprocal relationship between ECA and ICA blood flow control becomes apparent. As exercise intensity increases, there is an abrupt surge in ECA blood flow, while ICA perfusion paradoxically decreases (15). This hemodynamic redistribution appears to be selectively directed towards the face and skin vascular beds supplied by the ECA, suggesting a thermoregulatory mechanism to aid heat dissipation during high-intensity physical exertion (15). It is important to acknowledge other factors such as hyperthermia-induced alterations in CO_2 reactivity, cerebrovascular vasoconstriction, and hyperventilation-induced hypocapnia, can also contribute to a decrease in CBF (92–96). The dynamic regulation of blood flow through the ECA has also been shown to play a role during acute hypotensive events. During a bout of acute hypotension induced by thigh-cuff-inflation, both ICA and ECA blood flow decrease; however, in the recovery period back to baseline, ICA blood flow rapidly recovers, while ECA blood flow remains depressed (17). The prolonged reduction in ECA flow may suggest a dynamic regulation playing a key role in CA by redirecting blood to the brain, thereby supporting intracranial oxygenation and nutrient delivery (17).

While a growing body of research explores the redistribution of blood flow involving the ECA, experimental studies that have directly manipulated or modulated ECA blood flow control remain scarce. One method shown to modify ECA blood flow is via facial cooling. Facial cooling, can elicit a change in ECA blood flow where blood flow is decreased selectively for thermoregulatory purposes, and a decrease in ECA blood flow correlates to an increase in ICA blood flow (16). Another method that can potentially modify ECA blood flow is jaw clenching. The biomechanical action of jaw clenching can either increase resistance to facial arteries similar to any muscular contraction or induce a hyperemic effect at the cessation of activity; therefore, jaw clenching has the potential to contribute to hemodynamic changes to the extracranial vessel network. Jaw clenching involves the vascular components near and surrounding the neck and facial region. Previous studies have suggested that jaw clenching increases MCAv during jaw clenching (97). In extreme cases, jaw claudication is a severe form of jaw clenching and has been linked to severe ECA stenosis, necessitating a more detailed characterization of how the facial muscles impact extracranial blood flow control (98). There appears to be a very limited amount of research on the impact of jaw clenching on extracranial blood flow supply, which may be more relevant for the musculoskeletal etiology of jaw diseases.

It remains unclear whether the facial arterial network downstream of the ECA could serve as a viable target for experimental manipulation to control and divert carotid artery blood flow. While research has hinted the ECA plays a role in redistributing blood flow away from the ICA territory during physiological stresses, the feasibility and implications of actively manipulating the facial arteries to modulate this carotid blood flow diversion have not been directly addressed. The premise that it may be challenging to experimentally alter carotid blood flow due to the brain's protective autoregulatory mechanisms is reasonable based on current evidence. However, whether the facial arterial branches supplied by the ECA represent a valid

experimental approach to overcome this challenge and control carotid flow diversion remains an open question. While current research provides valuable insights into the ECA's role in redistributing carotid blood flow, it does not directly address whether the facial arterial network could be used as an experimental tool to control and divert carotid artery perfusion. This represents an area where further research is needed to determine its feasibility and potential implications for understanding cerebral hemodynamics and to better understand the consequences jaw clenching has on local blood flow control**.**

1.3 Current ultrasound methods to measure complex blood flow

Traditional Doppler ultrasound techniques are valuable for quantifying hemodynamic conditions and assessing peripheral arterial velocity, and flow volume (99). However, these techniques have limitations related to angle dependency and depth constraints, which hinder their ability to precisely depict and quantify intricate arterial hemodynamic patterns particularly in complex vascular regions like the carotid bifurcation (99). For instance, single-angle Doppler can only determine the direction of blood flow relative to the probe, which becomes problematic in areas where blood flows in multiple directions. To address these limitations, a novel vector flow imaging (VFI) technique has been developed, offering a more precise solution for visualizing and quantifying complex hemodynamic patterns (7).

VFI is an angle-independent ultrasound approach that enables the measurement and visualization of multidirectional blood flow velocities (31). It employs advanced techniques like transverse oscillation and high-frame-rate plane wave imaging to obtain flow vector information at higher frame rates, enabling a better depiction of complex flow dynamics (31). VFI can be used to assess hemodynamic alterations associated with carotid stenosis resulting from atherosclerosis by allowing the measurement of WSS and the identification of regions exhibiting turbulence and recirculation (31,100). Each individual vector in a VFI frame

represents directionality and absolute velocity values at a specific location (7). However, the interpretation of the VFI scan is far more detailed and comprehensive than that of Doppler-based techniques. Visually, the length of the arrows is directly proportional to the flow speed, with longer arrows corresponding to faster blood flow (Fig. 8) (31). The ability of VFI to provide an angle-independent, high-frame rate visualization and quantification of complex flow patterns has significant implications for diagnosing and monitoring vascular diseases. VFI captures full-field data, offering a comprehensive view of blood flow across an entire region. This capability enables the identification of complex flow patterns that are often indicative of pathological conditions, allowing clinicians to detect abnormalities that may not be visible with traditional imaging techniques (101). Additionally, VFI facilitates fine detail measurements within a single cardiac cycle, enhancing the precision of hemodynamic assessments (101).

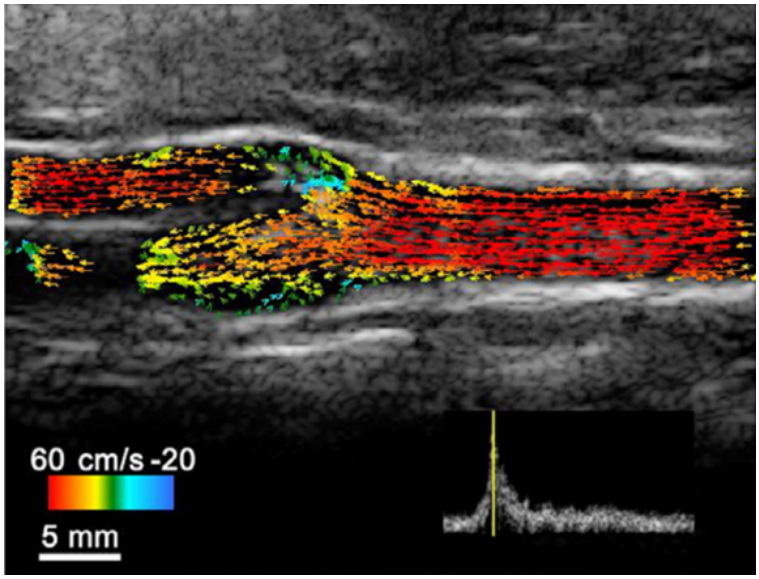


Figure 8: Vector flow image scan of the carotid bifurcation in a 23-yr-old male. Colour-coded arrows indicate the flow dynamics in different regions: red arrows point to areas of high blood flow velocity, yellow and orange arrows indicate regions of moderate flow, and green arrows represent areas with low flow. Retrieved from Au et al (117).

As previously mentioned, a common site for the development of atherosclerotic plaques is the carotid bifurcation due to its unique geometry and complex flow patterns (22,64). VFI is particularly well-suited for assessing blood flow dynamics at the carotid bifurcation. By

employing angle-independent methods, VFI can accurately measure and visualize blood flow velocities in all directions, overcoming the limitations of conventional Doppler ultrasound techniques (31). This capability is invaluable at bifurcations, where abrupt changes in vessel geometry and flow impingement give rise to complex, multidirectional, and turbulent flow patterns (31). Furthermore, VFI provides a more robust and intuitive visual representation of these intricate flow dynamics by displaying velocity vectors, streamline distribution, and vorticity distribution (31). In patients with carotid stenosis, the general pattern observed in VFI shows elongated velocity vectors. These vectors indicate that blood flow is accelerating as it passes through the narrowed lumen of the artery. The elongated nature of the vectors reflects the increased velocity of blood as it navigates through the constricted area, which is a common hemodynamic response to stenosis (31). Conversely, the velocity vectors are shorter in regions characterized by complex flow patterns, such as recirculation zones or areas of flow separation, indicating lower flow velocities and disturbed flow dynamics. These complex patterns suggest that blood flow is rarely smooth and laminar (31).

2.0 Study rationale

Experimentally altering carotid blood flow can be challenging since the brain's protective autoregulatory mechanisms take priority to ensure that sufficient blood is delivered to the brain. This makes it difficult to achieve or sustain desired changes in carotid blood flow, as the brain's need for stable blood flow overrides experimental manipulations. However, whether the facial arterial branches supplied by the ECA could provide a viable experimental approach to overcome this challenge and effectively control carotid flow diversion remains unclear. While previous research has attempted to influence ECA flow through indirect stimuli such as whole-body exercise and facial cooling, they do not directly address the potential of the facial arterial network as a tool for controlling carotid artery perfusion. The direct experimental manipulation of ECA flow has rarely been tested and it remains unclear how the carotid arteries reallocate flow in response to changing demands in the facial vasculature.

My research focuses on investigating how voluntary jaw clenching influences blood flow in both extracranial and intracranial vessels, with a particular focus on the carotid bifurcation. By examining changes in blood flow through the CCA, ICA, ECA, and carotid bifurcation, this work aims to understand how localized muscular activity in the facial region alters vascular dynamics.

By examining these effects, we aim to develop a method for predictably altering blood flow in the CCA, its branches, the ICA, the ECA, and the carotid bifurcation. Specifically, I seek to understand how blood flow patterns at the carotid bifurcation are modulated *in vivo* through selective changes in extracranial resistance, induced by voluntary jaw clenching. This approach offers a novel framework for studying extracranial and intracranial blood flow redistribution, with potential clinical relevance for understanding vascular adaptations associated with chronic jaw clenching behaviors in the dental field.

3.0 Research Questions and Hypotheses

Research questions

1. How does jaw clenching impact extracranial blood flow as measured at the ECA?
2. How does jaw clenching impact intracranial blood flow as measured at the ICA and the MCA?
3. How do blood flow patterns at the carotid bifurcation change as a function of flow diversions between the ICA and ECA?

Hypotheses

1. Jaw clenching will increase blood flow to the ECA leading to a redistribution of blood flow away from the ICA.
2. Jaw clenching will decrease intracranial blood flow as measured by ICA blood flow and MCAv, diverting more blood into extracranial pathways.
3. Jaw clenching will increase blood velocity and will result in greater disturbed blood flow as indicated by a decrease in the vector concentration coefficient measured with VFI.

4.0 Methods

4.1 Ethics

This study was reviewed and received ethics clearance through the University of Waterloo Research Ethics Committee (ORE # 45787). The research methods and protocols adhere to the recommendations outlined by the Declaration of Helsinki concerned with the use of human participants and this study was preregistered prior to beginning data collection in Open Science Framework (DOI 10.17605/OSF.IO/2VRS7).

4.2 Participants

Twenty-six healthy adults (age 19-32 years; 15 female) provided written consent and participated in this study. Prior to arrival, participants were asked to avoid strenuous exercise and alcohol for 12h, caffeine for 4h, and large meals for 3h before the testing session. All participants reported no documented history of musculoskeletal or cardiovascular disease or known medical conditions that would impact the health of the cardiovascular system. Exclusion criteria included current smokers, self-reported history of cardiovascular disease, respiratory disease, kidney disease, cerebrovascular disease, diabetes, musculoskeletal disorders; current medical prescriptions that impact the cardiovascular system or receipt of vaccine within 14 days prior to study start date; active pregnancy or pregnancy in the last 12 months, amenorrhea (absence of menstruation), or menopause. Individuals with known or expected bruxism and individuals who use nightguards were excluded from the study. Individuals with dental-related disorders such as chipped, cracked, loose, or missing teeth, periodontal disease, gingivitis, temporomandibular joint disorder, prior jaw injury, and tooth sensitivity that would prevent maximal jaw clenching activity were also excluded from the study. Lastly, those who were allergic to ethanol and silicone were excluded. Given the lack of research in this area, we did not have adequate information to power a sex-differences analysis.

4.3 Sample size calculation

A reasonable target effect size was determined for the isometric and dynamic jaw clenching conditions using G*Power (V.3.1; (102)). Multiple within-subject, paired Student's t-tests were employed to estimate the required sample size. Previous literature reporting ICA and ECA blood flow responses similar to our study's physiological conditions were selected to use as values for G*Power calculations. Data were extracted either directly from tables or, from figures using WebPlotDigitizer (103). Specifically, baseline ICA and ECA blood flow data were retrieved from Nakata et al (104). ICA blood flow for the isometric condition was determined by assuming an increase in MCAv is proportional to an increase in ICA blood flow since the ICA supplies blood flow to the MCA (97). ECA blood flow for the isometric condition was obtained from cardiovascular and cerebrovascular variables during isometric one-leg knee extensions (105). Lastly, for expected ICA and ECA blood flow changes during the dynamic condition, data was obtained during gum chewing tasks since chewing is a similar rhythm to dynamic jaw clenching (106). These values were then used to calculate Cohen's *d* effect sizes in G*Power for each comparison. ICA and ECA blood flow outcomes were analyzed separately for each protocol (isometric and dynamic jaw clenching), resulting in four distinct within-subject comparisons. The effect sizes were then used to estimate the sample size required for each outcome. The largest calculated sample size across these four outcomes was chosen to ensure sufficient statistical power across all primary analyses. *A priori* power analyses used an alpha level of 0.05, statistical power of 0.80, and an assumed correlation of 0.5 between repeated measures.

For the ECA, the calculated effect size for the comparison between baseline and isometric jaw clenching was $d = 0.65$, corresponding to a required sample size of n = 21 (Fig. 9), and the baseline to dynamic jaw clenching comparison yielded a very large effect size ($d =$

4.41), requiring only n = 3. For the ICA, the effect size for baseline versus isometric jaw clenching was $d = 0.79$ (n = 15), and for dynamic jaw clenching, $d = 5.26$ (n = 3).

The largest sample size required among all conditions (n = 21) was chosen to detect meaningful effects with high statistical power. This number was chosen to balance the need for statistical rigour with practical considerations, such as participant availability; however, due to the potential for data loss (e.g., incomplete datasets, participant drop-out, or technical issues), we increased the sample size by 20% then rounded up to the nearest even number to ensure an equal distribution between males and females. Therefore, 26 participants (15 females) were included in the study.

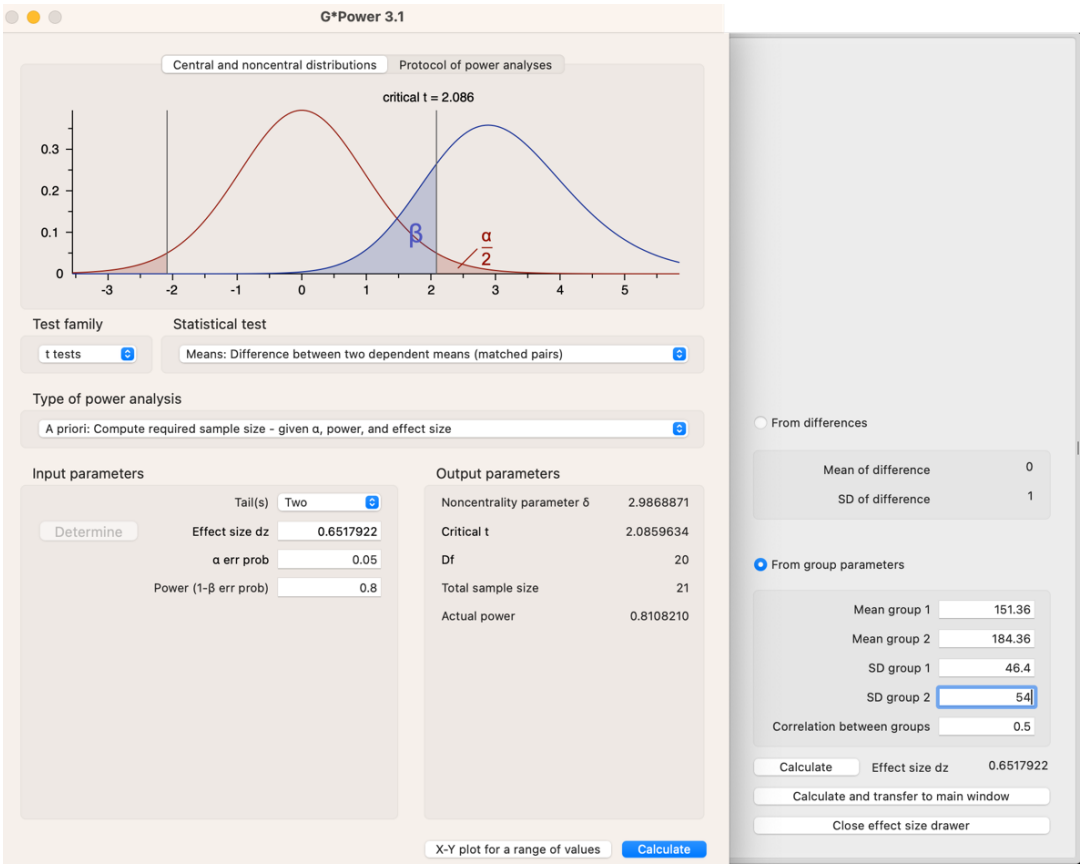


*Figure 9: G*Power analysis output for a paired Student's t-test comparing ECA blood flow at baseline (Mean group 1) vs during isometric jaw clenching (Mean group 2).*

4.4 Study Design

This study involved one 2 hr visit where participants performed a series of isometric and dynamic jaw clenching exercises, as well as a facial cooling intervention designed to elicit a non-metabolic vasoconstrictive response in the facial vasculature (Fig. 10). The position and posture of the participant can impact carotid and cerebral hemodynamics (107–109); therefore, we chose to have participants lay in the supine position for the entirety of the visit, with their head slightly tilted away from the sonographer. The supine position minimizes gravitational effects, while also providing optimal probe control for consistent, high-quality imaging of the right carotid artery. Upon arrival, participants were first required to perform a maximal intercuspal tooth clenching exercise characterized by the upper and lower teeth making full contact. Participants maximally bit on a mouthpiece connected to a bite force transducer that measures the overall occlusal force in Newtons (N), to determine their maximum voluntary jaw clenching force (MVJC). Each clenching effort was performed at least 3 times (3 seconds each) with 30-second breaks between each measurement and were then averaged to determine an average MVJC. Upon completing the MVJC, the participant was given a 5-minute resting period to ensure proper rest and recovery of blood flow and pressure. The experimental setup is illustrated in Figure 11.

Once the 5-minute recovery period concluded, the participant began a randomized protocol, starting either with isometric jaw clenching, dynamic jaw clenching, or facial cooling. The order of conditions was predetermined using a Williams Square Design to control for potential order and carry over effects. For the isometric condition, participants clenched their jaw at 25% of their MVJC and remained clenching for 60 seconds. Previous studies have reported a contraction force of 25% induces a hemodynamic response in the masseter muscle resulting in a large post contraction hyperemic response (110,111). This clench was performed four times since ultrasound images of the CCA, ICA, ECA, and carotid bifurcation were

recorded separately. A 5-minute resting period was given between each clenching effort. The dynamic condition required participants to perform an intermittent jaw clenching exercise, where the participant clenched their jaw at 70% of their MVJC for 3 seconds (ON) and then relaxed for 3 seconds (OFF). A 70% contraction force was selected to reflect a realistic and clinically relevant level of clenching typically experienced by patients with temporomandibular disorders (112). To ensure accurate timing of the clenches, a metronome was set to 3-second intervals, and participants were instructed to alternate between clenching and relaxing in response to each signal (113). This cycle was repeated continuously for a total of 60 seconds. Once again, this was performed four times, with a 5-minute resting period given between each clenching effort. During all resting periods, the mouthpiece was removed from the mouth.

The third aspect of the visit involved the application of a full-coverage facial cooling mask, omitting the ocular and oral areas. Cooling the face has shown to effectively reduce blood flow while minimizing the risk of excessive tissue hypoxia (114). The mask was cooled to 0.9 ± 1 °C and placed on the face. Participants were instructed to relax their facial muscles and refrain from jaw clenching. Ultrasound scanning began after the initial 5-minute cooling phase. The temperature of the face and mask were recorded approximately every minute until the scanning was complete, with the mask remaining in place throughout the protocol. When switching between each protocol, a 5-minute resting period was given. This allowed for physiological measures like heart rate and blood flow to return to baseline levels and provided the jaw muscles time to relax, preventing fatigue that may impact the following exercise protocol.

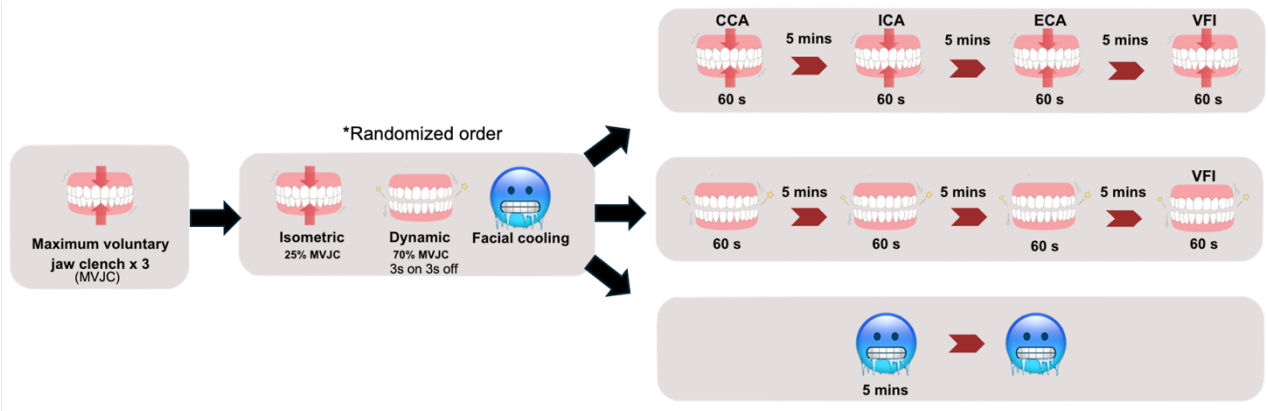


Figure 10: Timeline of study protocol. Participants were asked to avoid strenuous exercise and alcohol for 12h, no caffeine for 4h, and no large meals for 3h before each testing session. protocol. Continuous ultrasound recorded throughout clenching.



Figure 11: Participant experimental setup. Transcranial Doppler ultrasound probe was secured in place with a headpiece at the right middle cerebral artery. Electrodes were placed over the left and right masseter muscles to detect masseter muscle activity. The ultrasound probe was positioned on the right common carotid artery, and a bite force transducer was mounted above and in front of the participant's head to measure bite force.

4.5 Experimental measures

4.5.1 Data Acquisition

Central hemodynamics

A brachial blood pressure cuff was placed on the participants left arm to obtain duplicate blood pressure measurements at the beginning and end of each protocol, using an oscillometric device (CARESCAPE V100 Vital Signs Monitor, GE Medical Systems Information Technologies, Inc.). For the jaw clenching protocols, blood pressure was measured at the end of the fourth and final clench. A 3-lead electrocardiogram in lead II configuration was used continuously to capture timing and number of beats, time-aligned with ultrasound data.

Jaw clench

A commercial bite force transducer (Innobyte, Kube Innovation Inc., Montreal, QC) with a bilateral plastic mouthpiece attachment (INNOMP03) was used throughout the jaw clenching protocol to display real-time bite force results in Newtons (N). The mouthpiece provides accurate force readings within a 5% range across 0 to 2000 N (115). When participants bit down, the device displayed the total maximum bite force on the top row of the screen, while the left and right-side bite forces (relative to the mouthpiece) appeared on the bottom row. The device was positioned just above the participant's head at a comfortable height. For each jaw clenching effort, the mouthpiece was placed in the participant's mouth so that the upper molars aligned snugly with the cheek guards. During each resting period, the mouthpiece was removed. During both isometric and dynamic conditions, an assistant held down the capacitive sensing button on the device to provide live feedback, helping the participant maintain their target jaw clenching force. To ensure proper sanitation, a new disposable polyethylene cover was placed over the mouthpiece before each use. At the end of the jaw clenching protocol, the cover was removed and discarded, and the mouthpiece was thoroughly disinfected with a disinfectant wipe (CaviWipes, Metrex Research LLC, Romulus, MI, USA).

Electromyography

Electromyography (EMG) is a reliable tool used to indirectly estimate bite force. EMG is able to capture the electrical activity associated with jaw movements and allows for the assessment of muscular activity during various jaw clenching tasks (116). Therefore, EMG was used to evaluate muscle activation of the right and left superficial masseter muscles continuously throughout isometric and dynamic jaw clenching protocols. Self-adhesive surface electrodes (Kendall 130 Foam Electrodes, Cardinal Health, Dublin, OH, USA) were placed on the masseter muscles, anterosuperior to the angle of the mandible. Electrodes were connected using a three-surface lead (two recording electrodes and one reference) on the participant's left side, and a two-surface lead (two recording electrodes) on the right side, linked to the reference via a daisy-chain connection. To ensure proper placement of the electrodes, the participant was instructed to clench their jaw, and the investigator palpated the masseter muscle region with their fingers, located at the angle of the mandible, to confirm muscle activation and location (117). A reference electrode was then placed on the participants clavicle to serve as a common ground for the EMG recordings. EMG recordings were acquired using a four-channel preamplifier (ISO-4 Isolation Preamplifier, CWE, Inc. Ardmore, PA 19003, USA) and a four-channel electromyograph (BMA-400 AC/DC Bioamplifier, CWE, Inc. Ardmore, PA 19003, USA). Continuous data was sent to an acquisition device (PowerLab 8SP; AD Instruments Inc, Colorado Springs, CO) and commercial software (LabChart v7; AD Instruments Inc). Raw signals were amplified using a gain of 2000, and signals were band-pass filtered between 20-500 Hz.

Conventional Doppler Ultrasound

Ultrasound imaging was performed on the right CCA 2 cm proximal to the carotid bifurcation, while ICA and ECA scanning was done 1 cm distal to the carotid bifurcation to avoid complex blood flow patterns within the carotid sinus itself. Images were obtained using a standard

commercially available ultrasound unit with a 9L linear array probe (Vivid S70N; GE Medical Systems, Milwaukee, WI, USA). A 30s baseline blood velocity was recorded for each artery (CCA, ICA, ECA) prior to the initiation of the isometric, dynamic, and facial cooling protocols. Continuous blood velocity and arterial diameter measurements in duplex mode were then obtained during each jaw clenching effort and for 30s immediately following the cessation of jaw clenching. For the facial cooling protocol, measurements were recorded prior to face mask application and during the cooling stimulus. During the cooling phase, blood velocity and arterial diameter were measured with the mask in place at approximately 5 minutes into the protocol, with 30s recordings obtained for each arterial component. Since each artery was imaged separately, the imaging protocol was repeated three times per participant to capture the hemodynamic response at each location (CCA, ICA, and ECA). The Doppler sampling gate was adjusted to match the width of the vessel lumen by placing the calipers at the vessel walls to ensure accurate capture of blood velocity. Pulsed wave Doppler was angled parallel to the direction of blood flow, and the angle of insonation was consistently set to 60°. Artery depth ranged from 1–3 cm, and images were acquired at a frame rate of 9 frames per second.

Vector Flow Imaging

VFI was used to assess disturbances in blood flow patterns and to quantify flow uniformity via the vector concentration coefficient (VCC; (118,119)). The carotid bifurcation was imaged in the longitudinal plane using a 13-3 MHz linear array probe (Esaote SL1543) with a 4.3 cm width and interfaced with an open-platform ultrasound machine (US4r ultrasound, US4US, Warsaw, Poland; (119,120)). The bifurcation was positioned toward the left side of the screen to optimally visualize the CCA, carotid sinus, ICA, and ECA within a single window. If this was not feasible, the imaging plane was adjusted to ensure imaging of the CCA, ICA, and the carotid sinus. A custom vector Doppler sequence consisting of two transmit angles (10° and –10°) and three receive angles (10°, 0°, –10°) was used to estimate multi-angle blood velocity

vectors (119,121). Data were captured over ~4s intervals at an imaging depth of 4 cm and processed using previously established methods (118,119,122). Processing the data produced VFI estimates for production of vector projectile images (123) and VCC estimates which were used to assess flow uniformity within a selected region over time (124). VCC is calculated by first determining the flow angle (θ) of each velocity vector in the 2D field using the arctangent of its horizontal (vx) and vertical (vz) components (124). Each angle is then mapped onto the unit circle using $x = \cos(\theta)$ and $y = \sin(\theta)$ (124). The average of these x and y components is computed across all vectors, and the magnitude of the resulting mean vector gives the VCC (124). A VCC of 1 means that all flow vectors in the selected region of interest are aligned in the same direction (uniform), while a value of 0 reflects fully dispersed vectors and/or potential signal dropout from low flow velocities (119). The region of interest for the VCC was manually defined starting at the vertical point where the carotid bifurcation began (point where flow divider exists) and as far upstream as the image allowed (maximum 4.3 cm) tracing the carotid bifurcation. Data are presented as the time-averaged VCC value across three cardiac cycles.

Middle cerebral artery blood velocity

MCAv was continuously measured using TCD ultrasound (Doppler-Box™ e, Rev 4, Compumedics DWL, Singen, Germany) connected via Ethernet to a Windows-based computer running QL Monitoring Software (Compumedics DWL). A 2-MHz Doppler probe was positioned at the right temporal acoustic window to insonate the MCA. The MCA was initially located manually by the sonographer, and then the probe was secured using an adjustable headframe to maintain consistent insonation throughout the protocol. Micro adjustments were made as needed to optimize signal quality. The insonation depth was set between 40–60 mm with blood flow directed towards the probe (125) indicated by a bright, high-intensity red signal on the Doppler M-mode display. If the MCA was not successfully identified within the initial 10 minutes of setup, repeated attempts were made to locate the signal during resting periods

throughout the protocol to ensure data inclusion. Participants were instructed to minimize head movement during the protocol to maintain signal quality. If the probe was displaced, small micro adjustments were made during rest periods to re-acquire the MCA signal. Continuous data were recorded during baseline, jaw clenching efforts and facial cooling using an acquisition device (PowerLab 8SP; AD Instruments Inc, Colorado Springs, CO) and commercial software (LabChart v7; AD Instruments Inc). Due to limitations in available equipment, we were not able to measure end-tidal CO_2 using a capnograph. As a result, the analysis of this data will rely on existing literature to provide a robust theoretical framework and support the interpretation of our findings (97).

Facial Cooling

A full-coverage facial cooling mask omitting the ocular and oral areas was placed on the participant's face for no more than approximately 10 minutes. The mask was cooled in the fridge to 0.9 ± 1 °C and remained on the face for 10 minutes. The temperature of the facial skin was monitored using a temperature sensor (A Model 46 TUC Tele-thermometer, Yellow Springs, Ohio) where the probe was placed on the cheek to send continuous data to an acquisition device (PowerLab 8SP; AD Instruments Inc, Colorado Springs, CO) and commercial software (LabChart v7; AD Instruments Inc). The temperature of the mask was monitored every minute using a handheld infrared thermometer (SOVARCATE, Zhongshan, Guangdong, CN; temperature range: -50°C to 600°C; accuracy: ±2%).

4.5.2 Data Processing

Carotid artery blood flow

Arterial diameter for the CCA, ICA, and ECA along with blood velocity were analyzed from the stored cine loops retrieved from the conventional Doppler ultrasound. Due to incomplete data, n = 2 participants were excluded in the blood flow analysis. The diameter for each artery

was measured in triplicate at end-diastole using digital calipers to identify the interface between the intima and lumen. For the isometric condition, diameters were measured during baseline, mid-way (30s) through the clenching period, and during the post clenching period. For the dynamic condition, diameters were measured during baseline, during the ON and OFF clenching phases, and during the post clenching period. Lastly, diameters for the facial cooling condition were measured during baseline and during cooling after participants had worn the facial cooling mask for a minimum of 5 minutes. For each arterial diameter measured, a mean value of the triplicate measurements was recorded. Blood velocity was measured using an open-access MATLAB program (FloWave.US (126)), which calculates the mean blood velocity as the intensity-weighted average of the Doppler signal for each cardiac cycle (Fig. 12). Blood flow was then calculated as (127):

$$\text{Blood flow (mL/min)} = (\pi \cdot (\text{radius})^2) \cdot \text{ mean blood velocity} \cdot 60$$

Equation 1: Blood flow

Blood flow data was analyzed for each condition (baseline, clenching, post clench) separately, resulting in one measurement per artery per timepoint. Post-clench blood flow was calculated as the first 30-seconds after the cessation of clenching, reflecting both the hyperemic peak and subsequent elevation in blood flow. For the dynamic jaw clenching protocol, an additional step was taken to isolate and analyze blood flow during individual muscle contraction (ON) and relaxation (OFF) phases. In this case, each ON/OFF phase was treated as a distinct condition, allowing for the evaluation of intra-trial changes in flow across the dynamic task. Additionally, the PI was also calculated using the following equation for each artery and condition:

$$\text{Pulsatility Index} = \frac{Max\ (Vmean) - Min\ (Vmean)}{Mean(Vmean)}$$

Equation 2: Pulsatility index

Where Max (Vmean) represents the systolic mean velocity, Min (Vmean) represents the diastolic mean velocity, and Mean (Vmean) represents the average velocity across the cardiac cycle (128).

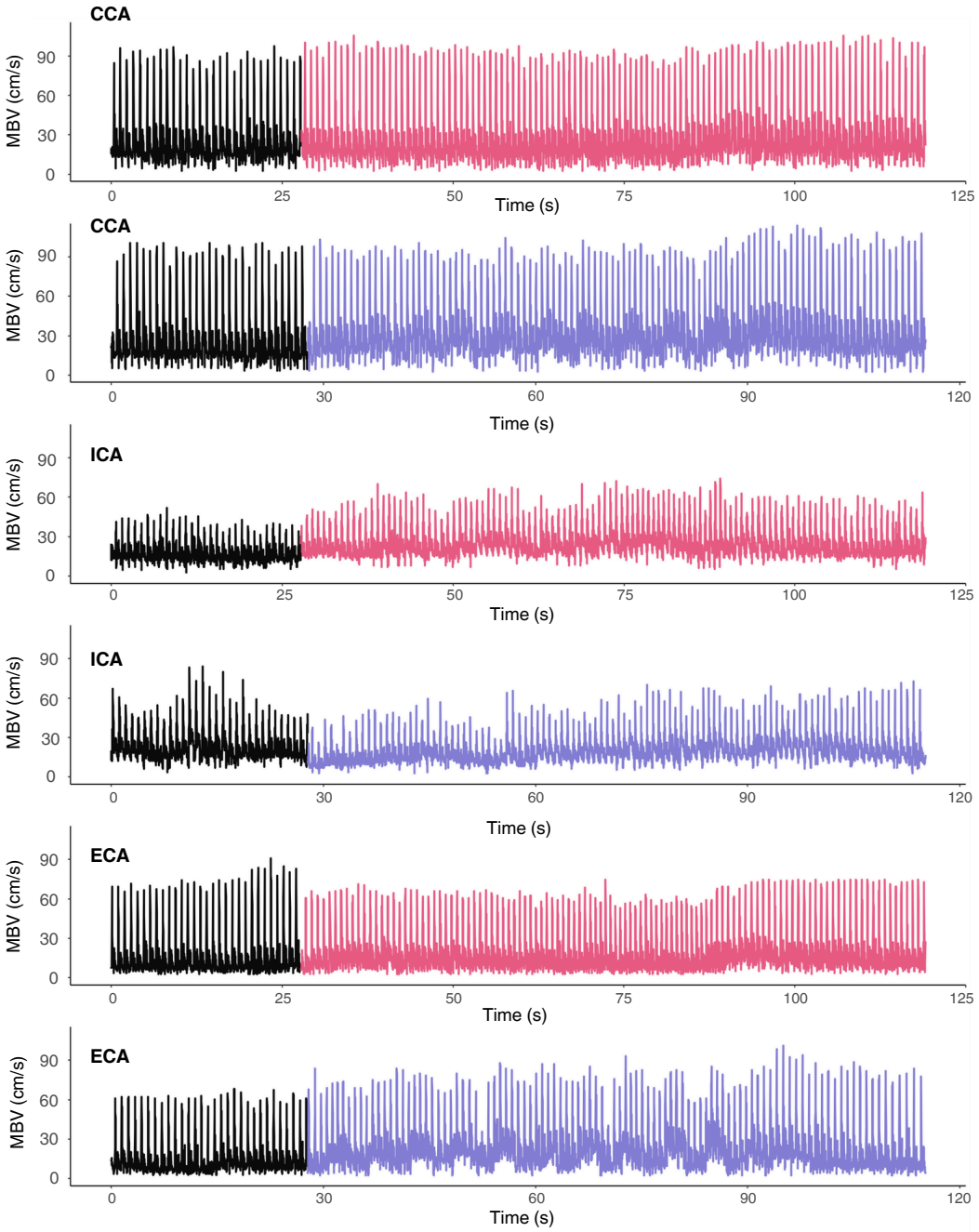


Figure 12: Raw mean blood velocity (MBV, cm/s) tracings from a 27-yr-old male during isometric (pink) and dynamic (purple) jaw clenching exercises. Data is shown for three arteries: CCA, ICA, and ECA For each artery, baseline, jaw clenching and post clenching data is plotted sequentially. Black line represents baseline MBV.

Middle Cerebral Artery Velocity

TCD data was continuously recorded at the right MCA and mean velocity signal (outer envelope) data were extracted from LabChart for average maximum and minimum cyclic values, as well as the mean MCAv for each condition and timepoint (Fig. 13). It is important to note that MCAv was derived from the outer envelope of the Doppler waveform, whereas ICAv was calculated as the intensity-weighted mean velocity. Therefore, differences in observed responses between MCAv and ICA blood flow should be interpreted with these methodological distinctions in mind. Various timepoints were extracted: baseline (30s prior to clenching or before applying the facial cooling mask), during each clenching effort or cooling phase, and 30s post-clenching. For the isometric jaw clenching protocol, data were extracted for the full clenching period, the first 10s, the last 10s. In the dynamic protocol, TCD data from all 11 clench efforts during the ON phase and all 10 rest periods during the OFF phase were extracted and averaged to generate representative ON and OFF values which was a similar approach used for blood flow analysis. Lastly, facial cooling data were extracted for 30s segments while the cooling mask was on the participants face.

Due to data dropout, n = 7 participants were excluded from this part of the analysis. Since each carotid artery component was imaged separately, jaw clenching efforts were repeated across four trials. However, only the first three trials were included in the TCD analysis, since the fourth clench focused on imaging the carotid bifurcation for VFI analysis, producing lesser quality TCD data.

Additionally, the Resistance Index (RI) was calculated as:

$$\text{Resistance Index} = \frac{PSV - EDV}{PSV}$$

Equation 3: Resistance index

,where PSV and EDV represent the peak systolic velocity and end diastolic velocity respectively (129). To generate a singular representative value for each condition, all outcome measures, including mean velocity and RI, were averaged across the three trials (CCA, ICA, ECA).

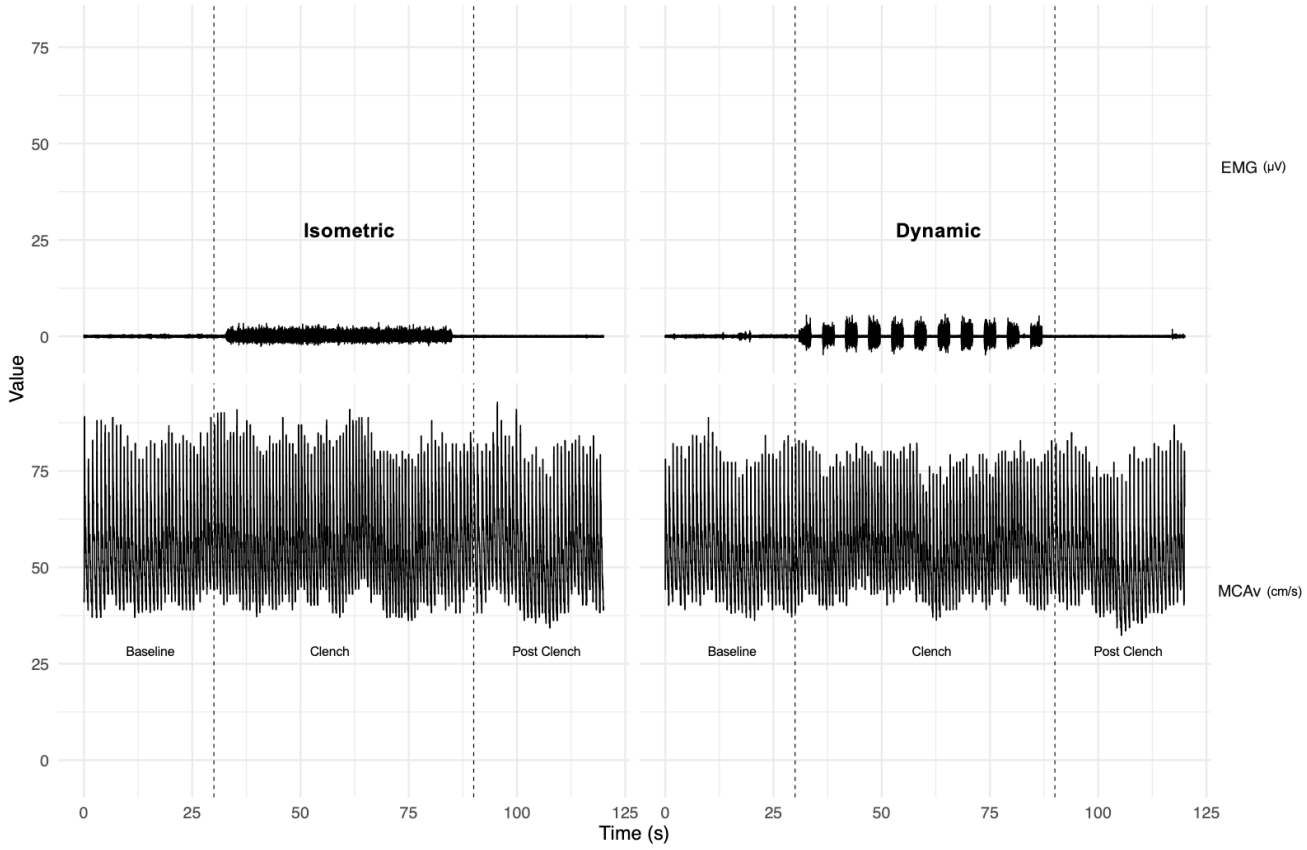


Figure 13: Raw tracings of right middle cerebral artery velocity and right masseter electromyography from a 24-yr-old male during isometric and dynamic jaw clenching.

Masseter Muscle EMG Activity

EMG activity was continuously recorded from the left and right masseter muscles throughout both isometric and dynamic jaw clenching protocols (Fig. 13). During each protocol, clenching efforts were repeated across four trials, since components of the carotid artery (CCA, ICA, ECA, and carotid bifurcation) were imaged separately. Although four clenching phases were performed per condition, only the first three were included in the EMG analysis since these clenches involved scanning each carotid artery component. The fourth clench was strictly associated with carotid bifurcation imaging using VFI and was therefore excluded from

masseter muscle activity analysis. The root mean square (RMS) is a measure based on the amplitude of the EMG signal, designed to quantify both the intensity and duration of muscle activation (130,131). Raw RMS values were exported from LabChart and organized in Excel for analysis. Due to poor EMG signal quality, n = 4 participants were excluded. For each participant, the average of the maximal RMS values from repeated MVJC efforts was determined.

For the isometric condition, raw RMS EMG data was extracted for the full 60-second clench, the first 10s, and the final 10s. For the dynamic condition, raw RMS EMG data for the first and last three clenches of each trial were averaged to represent the start and end phases, respectively. Masseter muscle activation was expressed as a percentage of RMS achieved during each participant's MVJC. For isometric jaw clenching, masseter muscle activation was based on the average RMS during the final 10s of the 60s clench. For dynamic jaw clenching, this value was calculated using the average RMS from the final three clenches. This calculation was done separately for each artery trial (CCA, ICA, ECA) and for both the left and right sides, then averaged to yield a single masseter muscle activation value per participant per condition. These values represent the relative activation level of the masseter muscle during each task, normalized to the participant's MVJC. Additionally, the fatigue index (FI) for each trial (side × artery) was calculated as:

$$\text{Fatigue Index (\%)} = \frac{Initial\ clench - Final\ clench}{Initial\ clench} \text{ x } 100$$

Equation 4: Fatigue index

Where initial clench and final clench refer to the raw RMS values at the beginning and end of each clenching trial (132). For the isometric jaw clenching, beginning and end were defined as the mean RMS during the first and last 10 seconds, respectively. For the dynamic jaw

clenching, beginning and end were defined as the average RMS across the first and last three clench repetitions. FI values were then averaged across arteries (CCA, ICA, ECA) and sides (left, right) to yield a mean FI per participant, per condition.

4.6 Statistical analysis

All quantitative analyses and graphing were performed in R (v4.4) (133). Blood flow and PI data were assessed using one-way repeated measures ANOVAs, with separate ANOVAs conducted for each artery (CCA, ICA, and ECA) and using timepoint as the within-subject factor (baseline, during clench, post clench). Additionally, MCAv, and RI data were assessed using one-way repeated measures ANOVAs, with separate ANOVAs conducted for each condition (isometric, dynamic, facial cooling) and using timepoint as the within-subject factor (baseline, during clench, post clench). A significance level of $\alpha = 0.05$ was applied for all statistical tests. Significant main effects were evaluated with post hoc pairwise comparisons using paired Student's t-tests with Holm's correction to identify specific differences between conditions. Specifically for the dynamic jaw clenching condition, since there were various ON and OFF phases, we averaged blood flow data across all ON and all OFF periods to generate summary values per subject. These were then analyzed using one-way repeated measures ANOVA with timepoint defined as: baseline, ON, OFF, and post clench, and then evaluated with post hoc pairwise comparisons using paired Student's t-tests with Holm's correction. For the facial cooling condition, blood flow, PI, MCAv, and RI were assessed using paired Student's t-tests for each artery to compare values between baseline and during facial cooling. Additionally, VFI outcomes were assessed solely for the voluntary jaw clenching conditions using paired Student's t-tests to compare values between baseline and post clenching for isometric and dynamic conditions.

As an exploratory analysis, paired Student's t-tests were conducted to compare which jaw clenching protocol elicited a greater increase in blood flow and to further examine redistribution specifically during the clenching phase. Additionally, a two-way repeated-measures ANOVA examined the effects of condition (isometric, dynamic) and timepoint (baseline, during clench, post clench) on percent blood flow distribution metrics (%ECA, %ICA, and ECA/ICA ratio) for the jaw clenching protocols. Significant main effects were then evaluated with post hoc pairwise comparisons using paired Student's t-tests with Holm's correction. Percent blood flow distribution metrics were calculated using the CCA blood flow measured during ultrasound imaging (Table. 3). These values were calculated as: %ECA = ECA/CCA, %ICA = ICA/CCA. It is important to note that CCA, ICA, and ECA flow values were not captured simultaneously during ultrasound imaging. This study acknowledges potential physiological variability between sequentially acquired CCA, ICA, and ECA flow measurements due to factors like heart rate and blood pressure changes. To quantify this, measured CCA blood flow was compared to estimated CCA blood flow (calculated as the sum of ICA and ECA flow), which resulted in a mean percent error of 5.03% ± 19.3%, suggesting that variability was relatively small under the conditions of this study. Significant main effects were then evaluated with post hoc pairwise comparisons using paired Student's t-tests with Holm's correction.

To investigate the potential relationship between masseter muscle fatigue, masseter muscle activation, and extracranial blood flow redistribution, Pearson correlation analyses were conducted to examine the relationships between the FI and masseter muscle activation with vascular redistribution metrics, including %ECA, %ICA, ECA/ICA ratio and absolute ECA blood flow during jaw clenching exercises. These analyses were performed separately for the isometric and dynamic jaw clenching conditions. To compare masseter muscle activation between jaw clenching conditions, a paired Student's t-test was conducted on the final percent

muscle activation values. Similarly, to assess fatigue, paired Student's t-tests were used to compare FI values between isometric and dynamic conditions across participants.

5.0 Results

5.1 Participant Characteristics

All participants successfully completed the protocol and adhered to the study requirements. Table 1 represents the participant characteristics for all who participated. Due to data dropout, participants were excluded from the varying components: blood flow: n = 2; TCD: n = 7; EMG: n = 4; VFI: n = 2.

Table 1: Participant characteristics

Variable	Male	Female	Total
N	11	15	26
Age (yrs)	25 ± 4	22 ± 2	24 ± 4
Height (cm)	180 ± 8	167 ± 10	172 ± 11
Body mass (kg)	81 ± 11	63 ± 11	71 ± 14
BMI ($kg \cdot m^{-2}$)	25.03 ± 3.01	22.5 ± 2.5	23.6 ± 2.9
MVJC (N)	813 ± 141	666 ± 119	734 ± 147
25% MVJC (N)	203 ± 35	167 ± 30	184 ± 37
70% MVJC (N)	569 ± 99	467 ± 83	514 ± 103

Data represented as means±SD. BMI, body mass index. MVJC, maximum voluntary jaw clench.

Table 2: Temperatures recorded during the facial cooling protocol.

Measurement	Pre-cooling temp (°C)	Temp at 5 mins (°C)	Post-cooling temp (°C)
Face	30.1 ± 2.0	23.5 ± 1.9	24.1 ± 1.6
Facial cooling mask	0.9 ± 1	8.9 ± 2.4	13.0 ± 3.5

Data represented as means±SD. Temp, temperature. The temperature of the facial skin was monitored continuously using a temperature sensor probe placed on the participants check, and the temperature of the mask was monitored every minute using a handheld infrared thermometer.

5.2 Carotid artery blood flow

During the isometric jaw clenching condition, CCA and ECA blood flow increased from baseline during both clenching and post clench phases ($p < 0.05$; Fig. 14A). ICA blood flow did not change during isometric jaw clenching ($p = 0.14$; Fig. 14A). The PI decreased for both the CCA and ECA during jaw clenching and post clench phases when compared to baseline (all $p < 0.05$; Fig. 15A) as well as decreased from clench to post clench ($p < 0.05$). In contrast, the ICA showed no change in PI throughout the isometric protocol ($p = 0.13$; Fig. 15A).

During the dynamic jaw clenching protocol, the average blood flow across all ON and OFF phases was analyzed. During both the ON and OFF phases, CCA and ECA blood flow increased, which remained elevated post clenching effort ($p < 0.05$; Fig. 14B) where blood flow was the greatest during the OFF phase compared to the ON phase ($p < 0.05$). Lastly, ICA blood flow increased post clenching compared to the clench phase during the ON phase ($p < 0.05$; Fig. 14B). PI decreased for both the CCA and ECA in the ON phase of the dynamic clenching protocol during the clench and post clench phases compared to baseline ($p < 0.05$; Fig. 15B). Additionally, ICA PI decreased during clenching and post clench phases ($p < 0.05$)

but increased from clench to post clench ($p < 0.05$; Fig. 15B). During the OFF phase, PI decreased in all three arteries during the clench and post clench phases when compared to baseline ($p < 0.05$) and increased from clench to post clench phases in all arteries ($p < 0.05$; Fig. 15B).

Lastly for the facial cooling protocol, there were no differences in blood flow observed across any artery ($p > 0.05$; Fig. 14C). The PI did not change for the CCA and ECA ($p > 0.05$), but the PI decreased for the ICA ($p < 0.0;5$ Fig. 15C).

The percentage of ECA blood flow (%ECA) increased during both clench and post clench periods compared to baseline ($p < 0.05$) for both isometric and dynamic conditions (Fig. 16). During isometric jaw clenching, the %ECA increased by 16.2% during the clenching period, and 36.8 % post clench. During dynamic jaw clenching, the %ECA increased by 19.1% during the clenching period and 47.9% post clench. Conversely, the %ICA decreased in both conditions. During isometric jaw clenching, %ICA decreased by 17.4% from baseline to post clench and by 12.6% from clench to post clench ($p < 0.05$). For the dynamic condition, %ICA decreased by 11.9% from baseline to post clench ($p < 0.05$; Fig. 16). The ECA/ICA ratio increased for both jaw clenching conditions during clenching compared to baseline by 36.0% for isometric condition and by 26.9% for dynamic condition ($p < 0.05$; Table. 3) and remained elevated post clench (67.7% isometric, 63.1% dynamic, $p < 0.05$), with isometric jaw clenching yielding a higher ratio overall than dynamic.

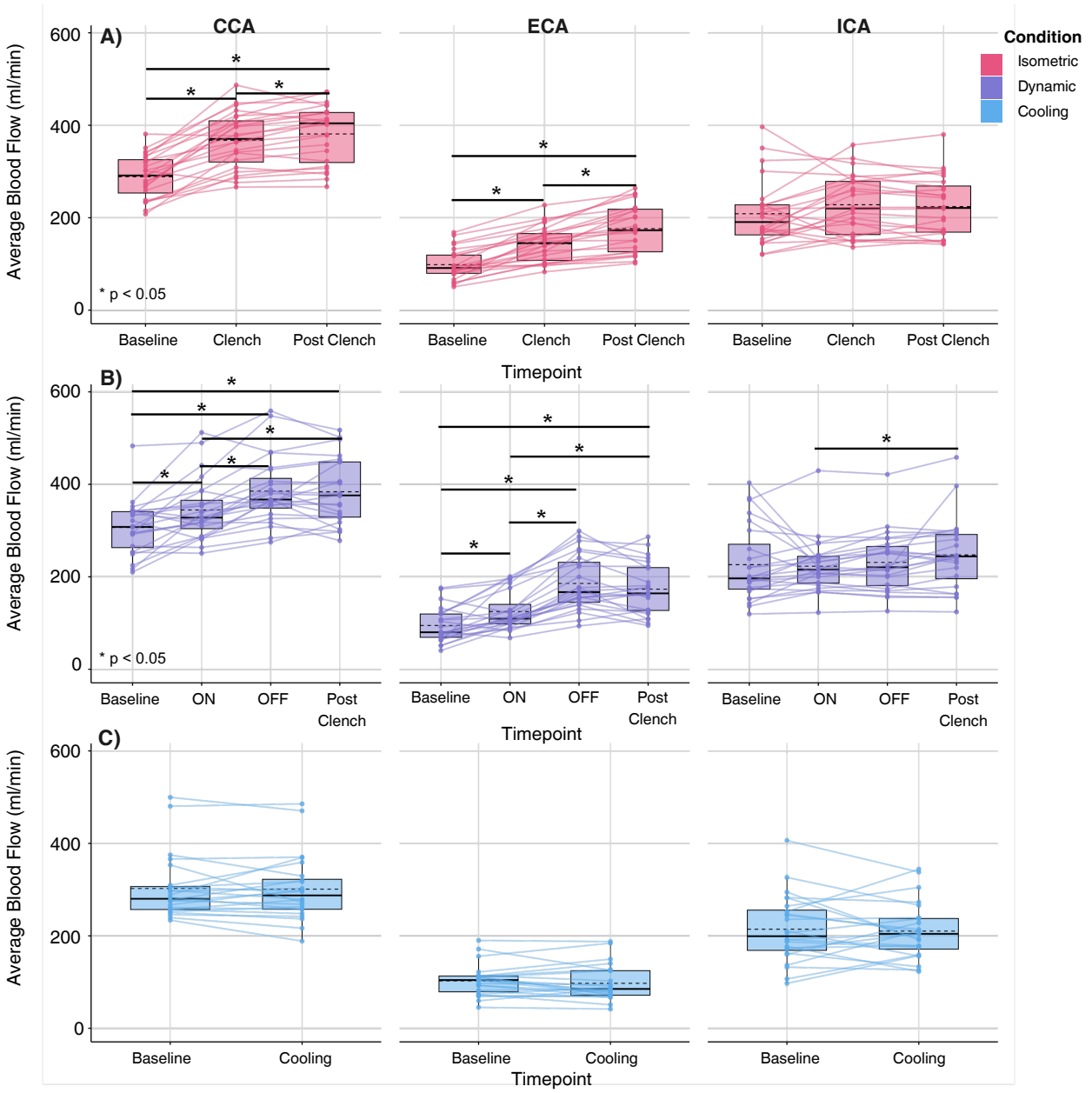


*Figure 14: Average blood flow in the CCA (first column), ECA (middle column), and ICA (right column) during isometric (A), dynamic (B), and facial cooling (C) conditions. Significant differences are represented as *p < 0.05. Individual participant values are overlaid as points, with lines connecting values across timepoints. Boxplots display the interquartile range, median (solid line), mean (dashed line), and whiskers display 1.5 times greater interquartile range. One-way ANOVA output represents Artery x Timepoint.*

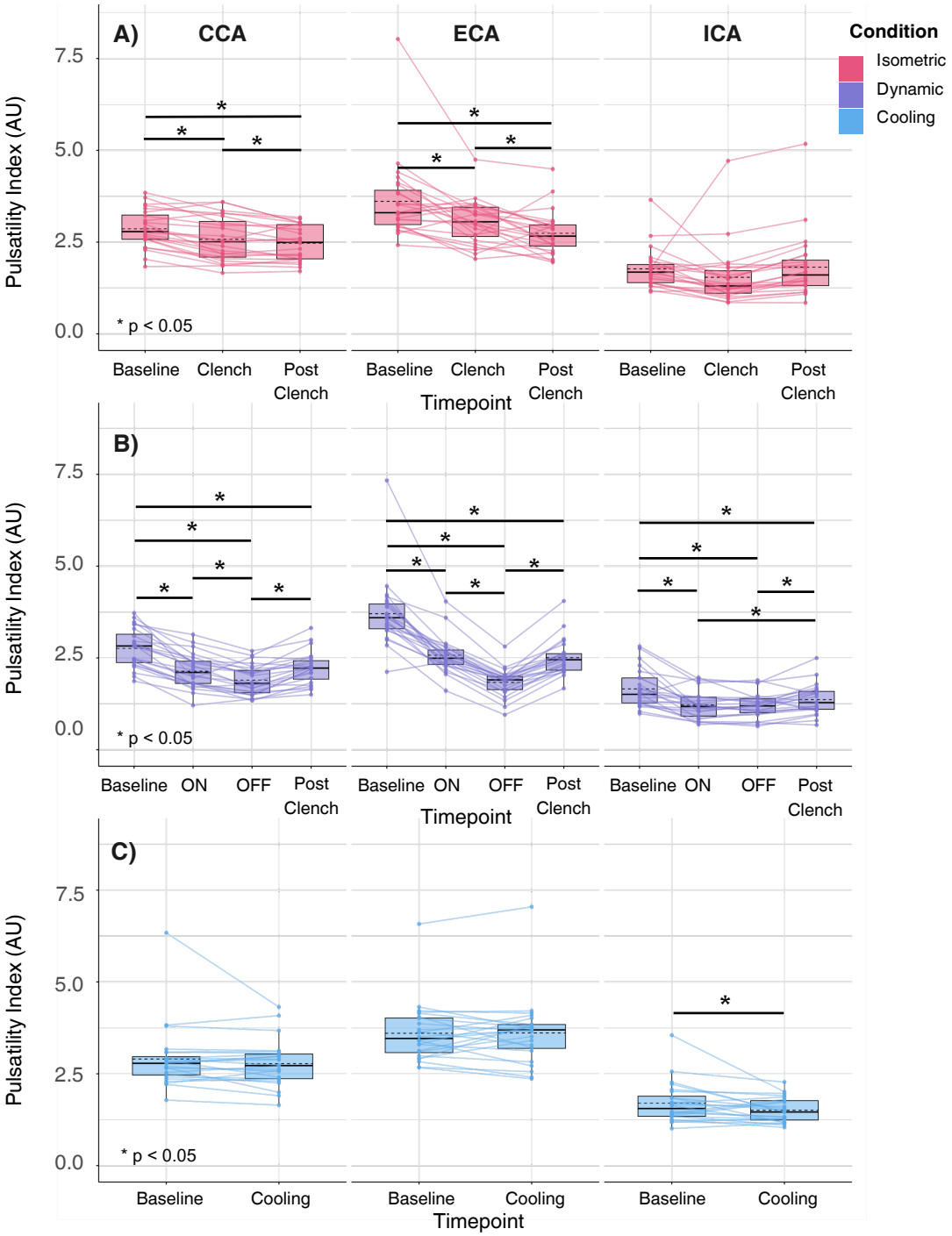


*Figure 15: Pulsatility index in the CCA (left column), ECA (middle column), and ICA (right column) during isometric (A), dynamic (B), and facial cooling (C) conditions. Significant differences are represented as *p < 0.05. Individual participant values are overlaid as points, with lines connecting values across timepoints. Boxplots display the interquartile range, median (solid line), mean (dashed line), and whiskers display 1.5 times greater interquartile range. One-way ANOVA output represents Artery x Timepoint.*

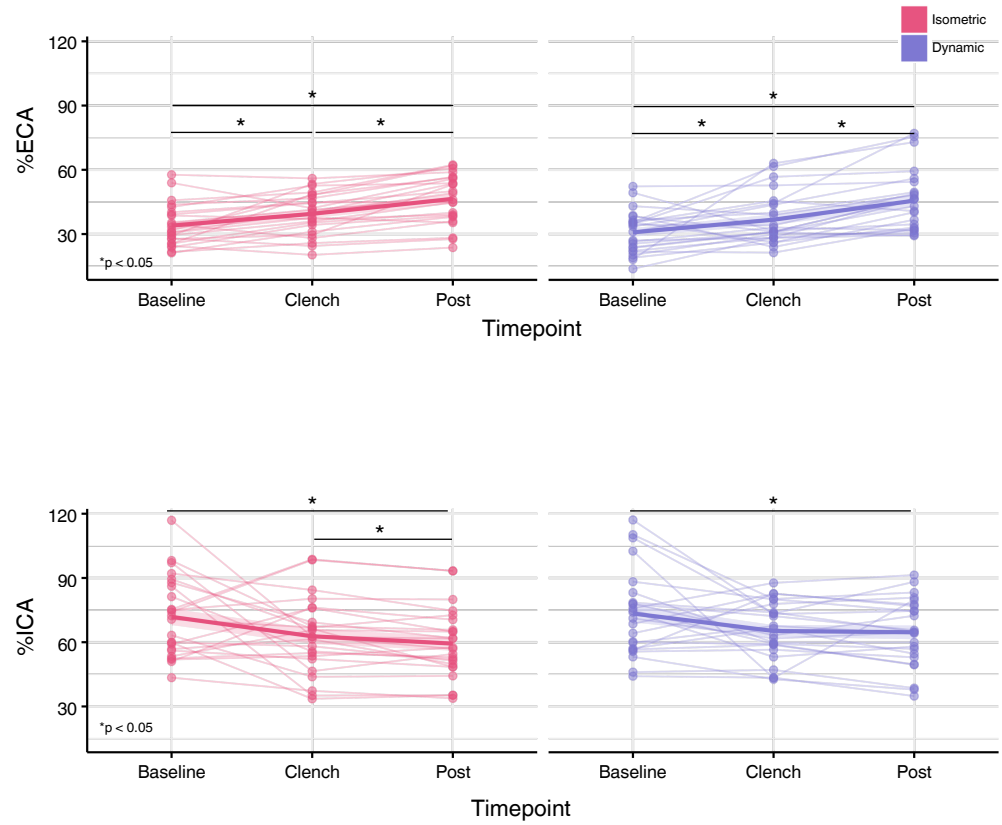


*Figure 16: Percent blood flow distribution metrics for dynamic and isometric jaw clenching. Thin lines represent individual participant responses. Thick lines indicate the mean trend across participants. Different colors indicate condition (Isometric = pink, Dynamic = purple). Significant differences are represented as *p < 0.05. Two-way repeated-measures ANOVA examined Condition x Timepoint.*

5.3 Middle Cerebral Artery Velocity

During the isometric jaw clenching protocol, there was a decrease in MCAv from clenching to post clench phases ($p < 0.05$; Fig. 17A). RI decreased during clench and post clench phases compared to baseline ($p < 0.05$) and increased when participants ended the clenching protocol ($p < 0.05$; Fig. 17B). During the dynamic jaw clenching protocol, MCAv increased during both ON and OFF phases compared to baseline ($p < 0.05$; Fig. 17A). Upon ending the clenching protocol, MCAv decreased compared to ON and OFF phases ($p < 0.05$; Fig. 17A). During both ON and OFF phases, the RI decreased compared to baseline ($p < 0.05$; Fig. 17B) and increased when participants ended the clenching protocol during the post clench phase compared to ON and OFF phases ($p < 0.05$; Fig. 17B). Lastly, there were no statistically significant changes in MCAv ($p = 0.88$) or RI ($p = 0.59$) for the facial cooling protocol (Fig. 17A and 17B).

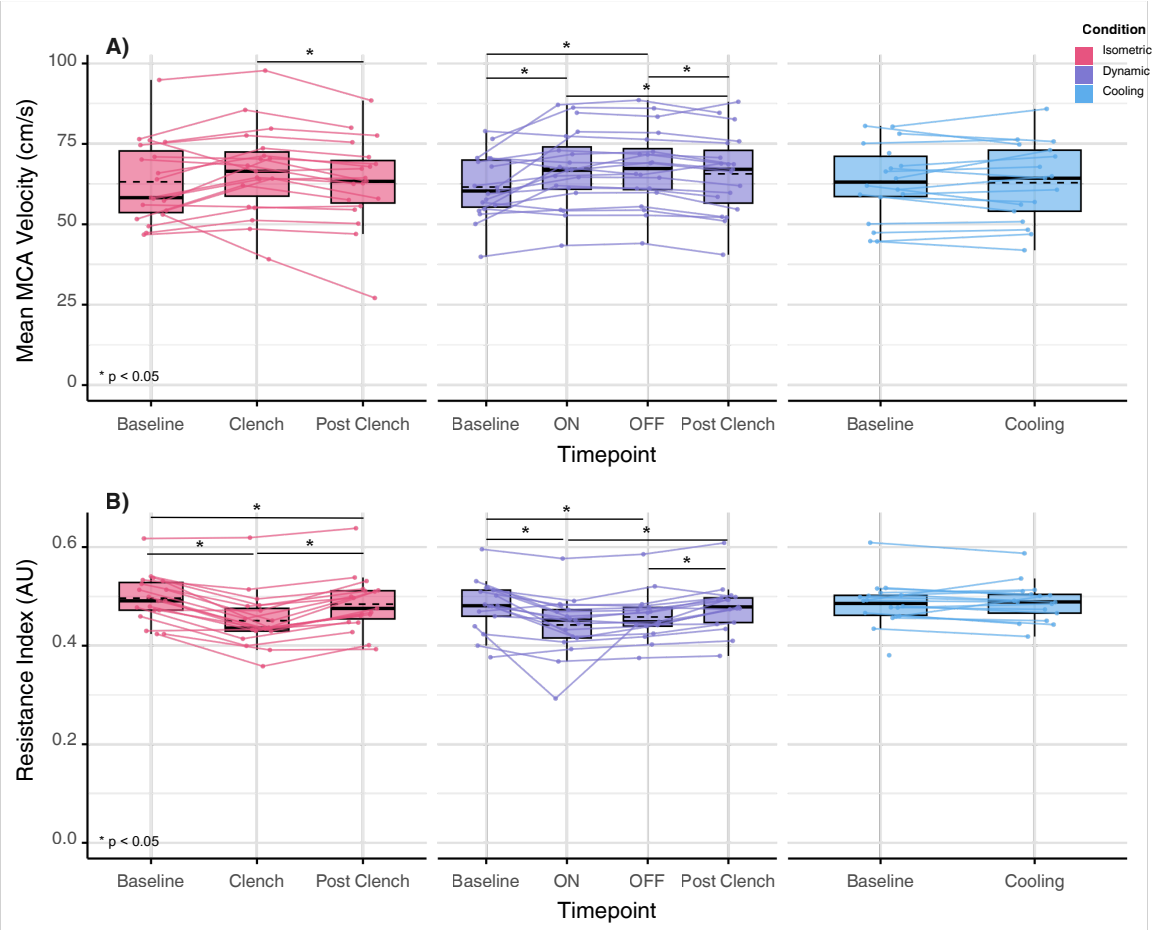


*Figure 17: Middle cerebral artery velocity (A) and resistance index (B) across all three experimental conditions for each timepoint (Baseline, Clench, ON, OFF, Post Clench, Cooling). Significant differences are represented as *p < 0.05. Individual participant values are overlaid as points, with lines connecting values across timepoints. Boxplots display the interquartile range, median (solid line), mean (dashed line), and whiskers display 1.5 times greater interquartile range. One-way ANOVA output represents Condition x Timepoint.*

5.4 Vector Flow Imaging

Qualitative assessment of VFI data revealed distinct flow characteristics at the carotid bifurcation during isometric jaw clenching consistent with the statistical findings (Fig. 18). Flow appeared fast and predominantly laminar at the section of CCA captured, reflecting increased velocity post clenching task. Near the flow divider, flow patterns became more complex and disturbed. Recirculation zones were observed near the ECA and ICA. The mean cycle VCC was calculated for three cardiac cycles. For the isometric condition, both the mean velocity and mean VCC increased post clench ($p < 0.05$; Fig. 19A and 19B). At baseline, the mean VCC was 0.43 ± 0.21 and increased to 0.55 ± 0.17 immediately after jaw clenching ($p <$

0.05). The mean velocity at baseline was 13.56 ± 12.61 and increased to 21.16 ± 6.78. There were no differences observed in the dynamic condition ($p > 0.05$; Fig. 19C and 19D).

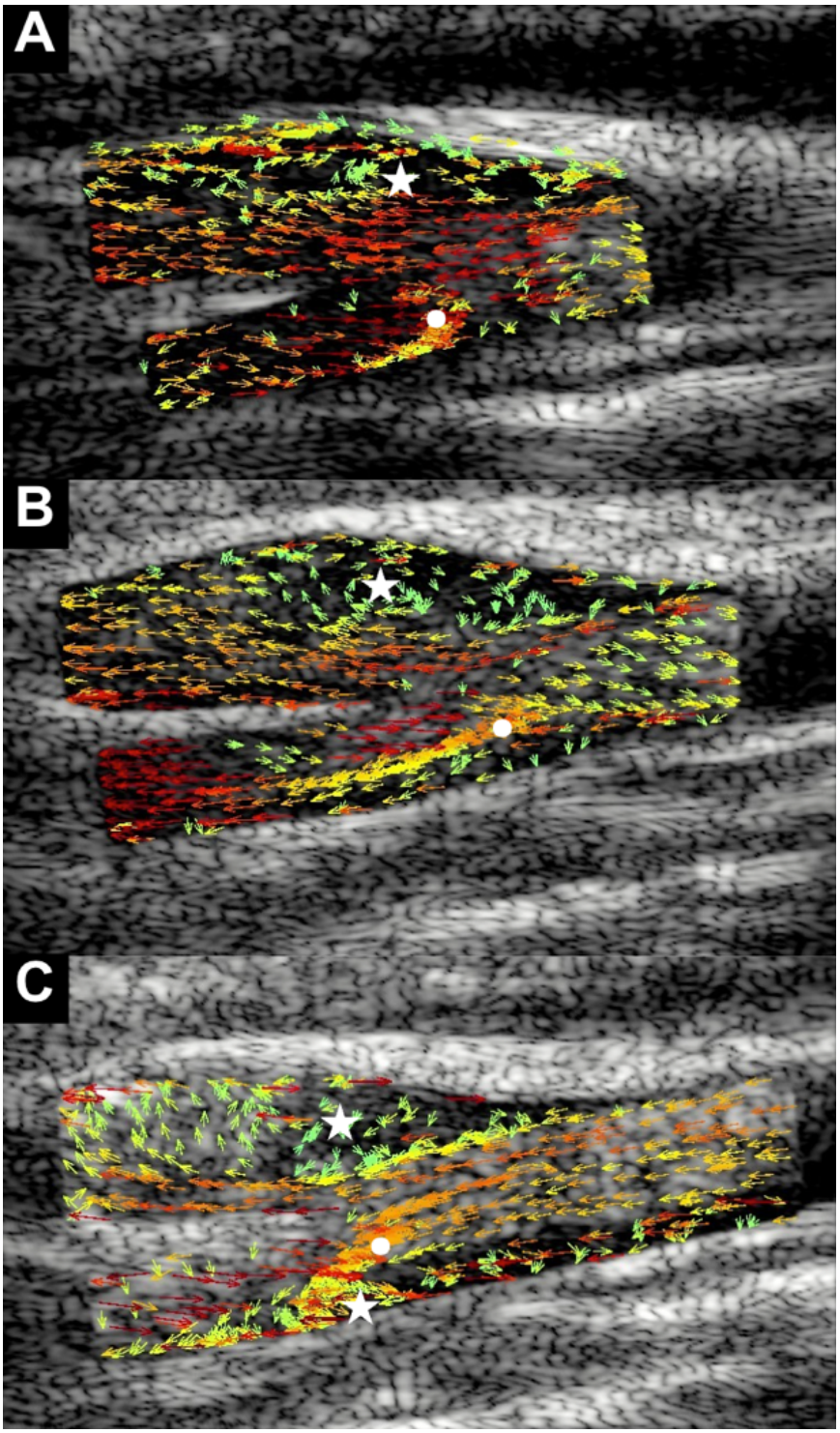


Figure 18: Representative qualitative vector flow images of the carotid bifurcation in a 27-yr-old male during baseline (A), and immediately post dynamic (B) and isometric (C) jaw clenching. All screenshots were captured during systole. Stars indicate regions of recirculation, and dots indicate regions of flow reversal. Colour-coded arrows represent flow velocity: green indicates low flow, yelllow and indicate moderate flow, and red indicates fast flow.

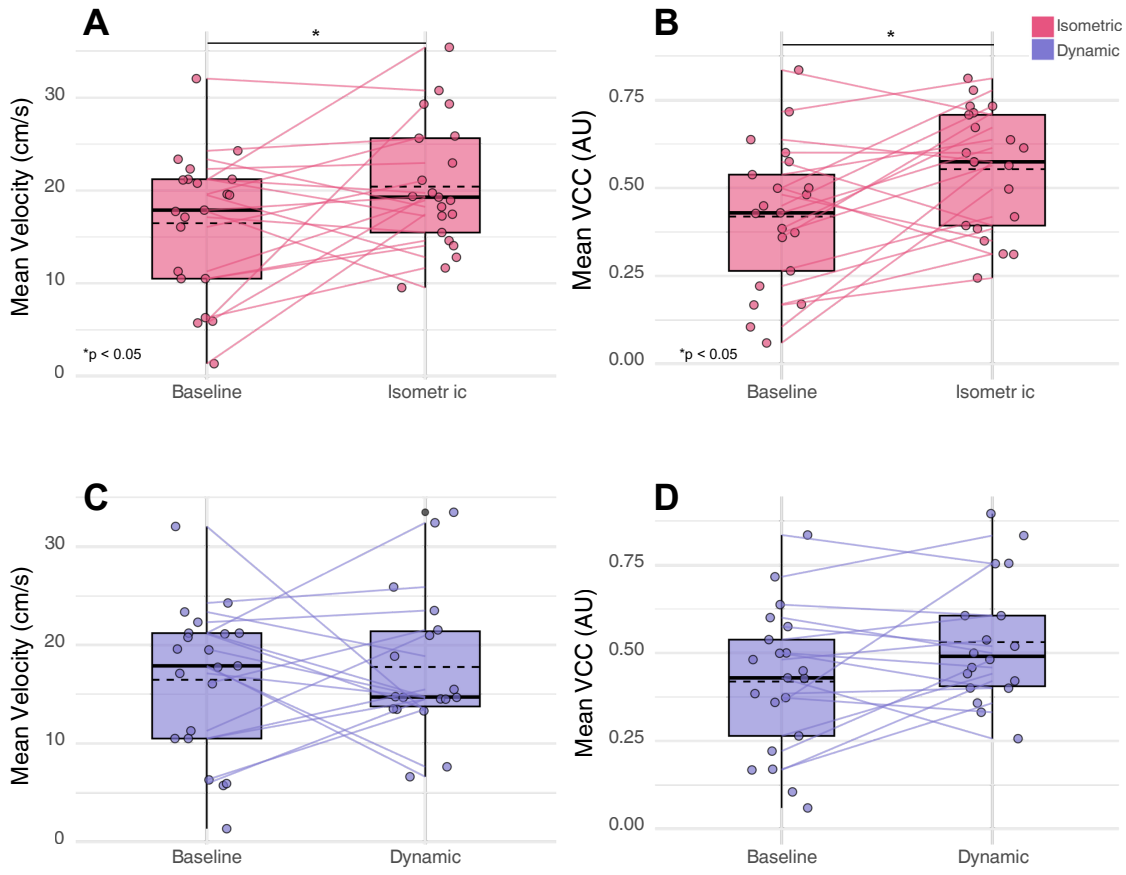


*Figure 19: Statistical analysis of vector flow imaging results during isometric and dynamic jaw clenching, comparing baseline to immediately post-clenching. (A) Isometric mean velocity; (B) Isometric mean VCC; (C) Dynamic mean velocity; (D) Dynamic mean VCC. Significant differences are represented as *p < 0.05. VCC, vector concentration coefficient. Individual participant values are overlaid as points, with lines connecting values across timepoints. Boxplots display the interquartile range, median (solid line), mean (dashed line), and whiskers display 1.5 times greater interquartile range. Paired Student's t-tests used to assess differences between baseline and post clench values.*

5.5 Electromyography

Masseter muscle activation was higher during dynamic jaw clenching compared to isometric jaw clenching (mean difference = 38.93%, $t(22) = 13.52$, $p < 0.05$). However, no difference was observed in the FI between conditions (mean difference = –6.89%, $t(22) = –0.52$, $p = 0.61$). Pearson correlation analyses revealed no relationships between masseter muscle activation or FI and blood flow redistribution metrics (%ECA, %ICA, or ECA/ICA ratio) during either isometric or dynamic conditions ($p > 0.05$).

Additional correlation analyses were conducted with ECA flow during both jaw clenching conditions. Results again revealed no associations. In the dynamic condition,

masseter muscle activation was not correlated with ECA flow ($r = 0.10$, $p = 0.66$), and FI was similarly unrelated to ECA flow ($r = 0.34$, $p = 0.12$). In the isometric condition, masseter muscle activation and FI were not correlated with ECA flow (activation: $r = 0.20$, $p = 0.36$; fatigue: $r = 0.27$, $p = 0.22$).

Table 3: Percent blood flow redistribution metrics during isometric and dynamic jaw clenching exercises.

Timepoint	% ECA	%ICA	ECA/ICA Ratio
Isometric			
Baseline	33.9 ± 9.7	71.8 ± 18.7	0.51 ± 0.21
Clench	39.4 ± 9.7*	62.8 ± 17.5	0.69 ± 0.32*
Post clench	46.4 ± 11.4*†	59.3 ± 16.1*†	0.85 ± 0.37*†
Dynamic			
Baseline	30.8 ± 9.8	73.4 ± 20.2	0.46 ± 0.25
Clench	36.7 ± 11.8*	65.2 ± 13.4	0.59 ± 0.24*
Post clench	45.6 ± 14.4*†	64.6 ± 15.9*	0.76 ± 0.33*†

Data represented as means±SD. *$p > 0.05$ vs Baseline, †$p > 0.05$ vs clench. ICA, internal carotid artery. ECA, external carotid artery.

Table 4: Cardiovascular, cerebral, and muscle activation responses across experimental conditions.

	Baseline	**Post Isometric Clench**	**Post Dynamic Clench**	**Facial Cooling**
Systolic blood pressure (mmHg)	110 ± 1	112 ± 10	111 ± 15	110 ± 11
Diastolic blood pressure (mmHg)	63 ± 1	65 ± 5	65 ± 5	63 ± 6
Heart rate (beats/min)	64 ± 1	65 ± 10	65 ± 11	65 ± 10
MCAv (cm/s)	63 ± 13	67 ± 14	68 ± 12	63 ± 12
EMG % Activation	-	28 ± 7	67 ± 15	-
Fatigue (AU)	-	3 ± 6	-4 ± 10	-

Data represented as means±SD. MCAv, mean middle cerebral artery velocity. EMG, electromyography.

6.0 Discussion

This research aimed to investigate how localized changes in facial vascular resistance induced by voluntary jaw clenching impacts extracranial and intracranial blood flow. Additionally, we examined whether voluntary jaw clenching increases disturbed flow at the carotid bifurcation due to flow redistribution between the ICA and ECA. Our findings show that voluntary jaw clenching increases blood flow to the ECA via an increase in CCA blood flow representing a shift in vascular demand toward the extracranial region. In contrast, blood flow toward the intracranial (ICA) region remained relatively unchanged, however, downstream increases in MCAv were observed. Overall, a larger percentage of blood flow was distributed to the extracranial region during voluntary jaw clenching. Additionally, at the end of isometric jaw clenching, the mean velocity of flow increased, and flow patterns at the carotid bifurcation became more uniform representing a reduction in disturbed flow as measured by an increase in the mean VCC. These findings suggest that during voluntary jaw clenching, the ECA does not act as a passive conduit but instead exhibits dynamic vascular responsiveness. Rather than diverting blood flow from the ICA, the increased ECA demand seems to be met by an overall increase in CCA inflow to support the heightened metabolic demand of the facial region. This supports the idea that extracranial vascular responses can meaningfully influence carotid hemodynamics without compromising cerebral perfusion.

6.1 Extracranial Blood Flow Response

Exercise hyperemia is a well-established physiological response where blood flow increases to meet the heightened metabolic demand of active muscle tissue (134,135). Activating the facial muscles through voluntary jaw clenching increased blood flow in both the CCA and the ECA. Since the CCA serves as the primary conduit supplying blood to both intracranial and extracranial regions (136), it plays a central role in supporting regional blood flow demands.

Previous research has shown that incremental cycling exercise increases blood velocity in the CCA, which directly accounts for an observed increase in CCA blood flow (15,136). In our study, this rise in flow is likely driven by localized muscular demand in the facial region through increased perfusion via the ECA. Since the ECA is the main branch supplying blood to the face, heightened demand in this region during voluntary jaw clenching likely prompted an increase in upstream CCA flow.

Interestingly, despite increases in CCA and ECA blood flow, vessel diameters did not change. The observed hyperemia was not due to passive dilation of the large vessels, but more likely driven by reductions in downstream vascular resistance. Supporting this, we observed a decrease in the PI during jaw clenching in both the CCA and ECA. The PI is a measure of vascular resistance, calculated from the difference between systolic and diastolic velocities relative to mean velocity (41). Since blood flow and vascular resistance are inversely related (137), the drop in the PI suggests that resistance in the CCA and ECA decreased, allowing more blood to flow to the facial region in response to a heightened metabolic demand of the facial muscles. Our findings suggest that the clenching-induced rise in blood flow in the CCA and ECA was actively accommodated by changes in resistance, not vessel diameter.

Previous studies have shown that ECA blood flow increases by as much as 42% during whole-body exercise, and remains elevated after completing the exercise (138). This response is commonly attributed to thermoregulatory demands to help dissipate heat from the head and facial region through enhanced extracranial perfusion (15,139). Similarly, our study supports the idea that ECA blood flow increases and stays elevated following facial exercise. However, in our case, this response is driven by localized muscular demand. Specifically, activating the facial muscles through voluntary jaw clenching triggered an increase in ECA blood flow. There is limited research directly linking jaw clenching to carotid artery blood flow; however, studies have explored changes in blood flow to the facial region, particularly in the masseter muscle,

during various jaw clenching tasks (111,140,141). A study using ^{133}Xe clearance found that isometric jaw clenching at approximately 50% max EMG increased masseter blood flow during the task, but there was a 27 times greater increase in blood flow post clenching effort compared to the initial resting flow values (142). This suggests the masseter muscle's oxygen demand temporarily exceeds its blood supply during jaw clenching, leading to a rebound in blood flow post-task. Even as little as a 5% MVJC can elicit a post clench hyperaemic response (111). These findings confirm that facial muscle activation alters local hemodynamics with a rebound increase in perfusion once clenching ceases. While most studies focus on changes in blood flow post clenching, our study builds on this by showing changes in blood flow that are occurring both during and after jaw clenching. ECA blood flow increased during jaw clenching and continued to stay elevated post clenching. This suggests that jaw clenching creates an immediate metabolic demand in the masseter muscle that is met by upstream flow from the ECA. Although we did not directly measure intramuscular perfusion in the masseter muscle, previous work showing masseter hyperaemia after jaw clenching supports the idea that localized muscular demand contributes to the observed changes in ECA blood flow (140,143). This reinforces the ECA's role in dynamically responding to both the active and recovery phases of facial muscle use.

6.2 Intracranial Blood Flow and Cerebrovascular Response

Despite observing changes in ECA blood flow, ICA blood flow remained relatively stable across both jaw clenching conditions; however, there was an increase in ICA blood flow post clenching in the dynamic condition. Changes in CBF during exercise are driven by multiple factors, including systemic cardiovascular responses and neural activation specific to the task (97). Isometric jaw clenching was relatively low in intensity, and there were no notable changes in blood pressure or heart rate. Since increases in perfusion pressure are typically needed to

drive CBF adaptations (144), it is not surprising that ICA flow remained stable in our study. The present findings are consistent with prior research where one study had participants perform low intensity isometric handgrip exercise at 25% of their maximum voluntary contraction, the same relative intensity as our jaw clench, and found no significant changes in ICA velocity post exercise (145). This suggests that at lower intensities, the stimulus may simply not be strong enough to require redistribution between the ICA and ECA or provoke noticeable changes in ICA blood flow. In contrast, dynamic jaw clenching elicited an increase in blood flow post clenching when compared to the ON clenching phase. Dynamic jaw clenching involves coordinated, rhythmic movements characterized by repeated activation and relaxation similar to mastication (146,147). Mastication has shown to increase CBF in different regions of the brain (147), therefore, the repeated cycles of muscle activation and relaxation may increase the overall metabolic demand and, in turn, stimulate greater perfusion to meet this demand since this was also performed at a greater intensity (70%). The present study supports the idea that dynamic, higher-intensity jaw clenching perhaps is more effective in stimulating CBF than low-intensity isometric jaw clenching.

Although ICA flow remained relatively stable, there were observable changes in the ICAs PI where overall the PI decreased (Fig. 12B). Although the PI can reflect cerebrovascular resistance, it is also influenced by factors such as cerebral perfusion pressure and arterial compliance (42,148,149). Changes in the PI may have reflected shifts in distal cerebrovascular tone or microvascular dynamics that occurred independently of changes in bulk ICA blood flow. A similar finding was found during dynamic cycling exercise, where the PI increased despite no change in ICA flow (150). Since voluntary jaw clenching is a relatively small muscle activity, it may only be selectively increasing blood flow in localized higher brain regions related to jaw motor control.

Jaw clenching stimulates various regions of the brain particularly those involved in motor execution, proprioceptive feedback, and sensorimotor integration (151). Regions include the primary motor and somatosensory cortices, premotor cortex, supplementary motor area, inferior frontal gyrus, insula, and the basal ganglia (151). Conveniently, these regions are largely supplied by the MCA (84), therefore, activation of these regions during voluntary jaw clenching in our study could have elicited a regional cerebrovascular response where changes were localized to these specific vascular territories. This could explain the changes observed in MCAv despite no changes in ICA blood flow. During dynamic jaw clenching, there was an increase in MCAv. Given that dynamic jaw clenching was performed at a higher intensity (70% MVJC) than the isometric condition (25% MVJC), the observed increase in MCAv aligns with previous research suggesting that both the intensity and pattern of muscle contraction influence cerebrovascular responses and activation patterns (97,151). For example, stronger muscle contractions elicit greater neural excitability, and clenching tasks that involve all teeth, especially the molars, have been shown to generate more widespread cortical activation than those using only the front teeth (152,153). Hasegawa et al. further supports these findings since MCAv increased during jaw clenching and chewing, but not during tooth-tapping (a weaker stimulus), highlighting the importance of task-specific motor engagement and effort (97). Moreover, repeated jaw clenching has been shown to induce neural plasticity and increased excitability (154), reinforcing the idea that the observed cerebrovascular changes reflect neurovascular coupling rather than systemic hemodynamic shifts. It is important to note that fluctuations in arterial CO_2 can impact MCA diameter (87,88), and that changes in velocity should be interpreted with caution when CO_2 levels aren't stable (89). We based the present study's approach on the study conducted by Hasegawa et al. (97), where transcutaneous CO_2 stayed within the normal physiological range (37–45 mmHg) during similar jaw clenching tasks. Therefore, it was assumed that MCA diameter likely stayed stable in the present study.

The changes in MCAv observed are reflected in the changes observed in the RI calculated. There is an inverse relationship between CBF and RI where when CBF increases, the RI decreases, and vice versa (155). Typically, at low exercise intensities, increases in cerebral blood velocity are accompanied by rises in RI suggesting that distal vessels maintain or increase resistance, limiting blood flow (156). In contrast, at higher intensities, RI decreases as vessels dilate, reducing resistance and allowing CBF to increase (156). In our findings, the RI decreased during both dynamic and isometric jaw clenching conditions, indicating a reduction in downstream cerebrovascular resistance. This suggests that downstream vasodilation occurred to accommodate increased flow during jaw muscle activation. However, RI increased during the post clenching phases for both conditions, reflecting a likely downstream vasoconstrictive or autoregulatory rebound once jaw clenching ceased. This pattern underscores the dynamic regulation of cerebral vascular tone in response to varying neural and hemodynamic demands during and after jaw clenching.

Collectively, these findings suggest that although voluntary jaw clenching does not appear to trigger widespread changes in CBF, it may still lead to localized increases in perfusion within task-relevant brain regions. This effect was particularly evident during dynamic jaw clenching, where MCAv changes were more pronounced. These localized responses likely reflect neurovascular coupling driven by task-specific neural activation and motor engagement, rather than systemic hemodynamic changes.

6.3 Blood Flow Redistribution

Although the ICA and ECA originate from the same vessel, their functional roles and regulatory mechanisms respond differently to physiological stress (15–17,157). The ICA is tightly regulated and maintains relatively stable cerebral perfusion across a range of systemic pressures through mechanisms like autoregulation, CO_2 sensitivity, and neurovascular coupling

(158). In contrast, the ECA is generally considered a pressure-passive vessel, more susceptible to systemic hemodynamic changes and less tightly controlled (10–12). During exercise, several studies have shown that ECA blood flow and vascular conductance increase, while ICA blood flow remains unchanged due to a reduction in ICA conductance (157,159). This supports the idea that the ECA acts as a modifiable outlet, helping buffer cerebral perfusion during transient hemodynamic challenges and allows the ICA to maintain its tightly regulated function (10,17).

By engaging the facial muscles through voluntary jaw clenching, we elicited localized metabolic demand in the facial region that led to a direct increase in ECA blood flow without substantial systemic cardiovascular engagement. This indicates that the ECA responds dynamically to the metabolic needs of active facial muscles. These findings highlight the capacity of extracranial vessels to adjust flow in response to local demand and reinforce the idea that facial muscle activity can modulate upstream carotid dynamics in a controlled, localized way.

Although we did not observe a clear redistribution in blood flow between the ICA and ECA, we were curious whether the type of jaw clenching exercise influenced both the magnitude of blood flow and the redistribution of flow between the carotid branches to some degree. An exploratory analysis was conducted of relative flow metrics specifically %ECA, %ICA, and the ECA/ICA ratio across isometric and dynamic clenching conditions. It is well-known that the ICA receives the majority of blood flow receiving approximately 70% of total CCA output, whereas ECA flow will receive the remaining 30% (160). However, during high-intensity dynamic exercise, these percentages shift and there is a redistribution of blood flow where blood flow is favoured to the extracranial region (15). In our study, there was an increase in %ECA during both jaw clenching conditions, alongside a decrease in %ICA, indicating a shift in blood flow toward the extracranial circulation. This was further supported by observing an increase in the ECA/ICA ratio indicating more blood flow from the CCA is being delivered

to the extracranial region (ECA) (161). While dynamic jaw clenching elicited greater masseter muscle activation, as expected given the higher relative intensity (70% MVJC), this did not translate to greater ECA blood flow. In fact, isometric jaw clenching, despite involving lower EMG activation, yielded a higher increase in ECA blood flow during active jaw clenching and an overall greater ECA/ICA ratio. These findings can likely be explained by the distinct mechanical and vascular demands of each task. Isometric contractions involve sustained muscle contraction, which increases intramuscular pressure and can compress local vessels, limiting blood inflow (162). In our case, the facial vasculature may prioritize perfusion during sustained contraction in order to maintain local oxygen delivery (162), hence blood flow going through the ECA increases to supply the facial region. In contrast, dynamic jaw clenching is phasic, alternating between brief contractions and periods of relaxation. During contraction, there is still some vascular compression, but the intermittent relaxation allows for periodic surges in flow.

Interestingly, there was no relationship between EMG-derived FI and these percent blood flows. While limb muscle studies consistently show that muscle fatigue can limit perfusion due to mechanical compression or metabolic buildup, they also demonstrate that fatigue often elicits proportional increases in blood flow as a compensatory mechanism to meet rising metabolic demand (135,163). Our findings do not support this; however, they do align with prior work on the jaw-closing muscles, which may behave quite differently. Clark and Carter (164) reported that the jaw muscles, particularly the masseter and temporalis, demonstrate an unusual resistance to contractile fatigue, even under sustained isometric loads. They found no reduction in bite-force capability or peak EMG and suggested that participants often stopped clenching due to discomfort rather than true fatigue (164). This has been attributed to factors such as higher capillary density, better oxygenation, and a predominance of fatigue-resistant type I fibers within the masseter and deep temporalis muscles (165,166). In

our study, the absence of any relationship between FI and blood flow may reflect this same phenomenon, rather than muscle fatigue driving blood flow, it is the mechanical nature of the task (sustained vs dynamic) that shape the hemodynamic response.

6.4 Blood Flow Patterns

A key aim of this study was to investigate how blood flow patterns at the carotid bifurcation change as a function of flow diversions between the ICA and ECA. Our findings found that post isometric jaw clenching increases both the velocity and the VCC at the carotid bifurcation, suggesting that blood flow did not become more chaotic or disturbed, but rather became coherent and laminar in nature.

Blood flow patterns at the carotid bifurcation are well-known to be complex exhibiting patterns such as zones of recirculation, areas of flow separation, and turbulent flow (31,55). Specifically retrograde flow from the ECA into the ICA, is considered a common phenomenon that is influenced by the geometry of the carotid bifurcation (46,55,56). Qualitatively assessing our VFI results, as expected, there are recirculation zones occurring at the flow divider between the ICA and ECA (56). Given that our blood flow analysis showed an increase in flow directed to the ECA during isometric jaw clenching, future research should more closely examine flow patterns within the ECA under similar physiological conditions to identify if flow is becoming more disturbed. Interestingly, the overall acute hemodynamic response observed in our study revealed that isometric jaw clenching increased flow uniformity, as indicated by increased VCC values post jaw clenching. This reflects a more homogeneous velocity profile across the bifurcation and likely retains laminar characteristics and does not necessarily indicate disturbed or turbulent flow. It is important to note, however, that the VCC quantifies flow alignment but not the direction in which it is aligned (119).

In acute settings, increased velocity and increased flow uniformity may be beneficial, as it helps reduce regions of low or oscillatory shear stress, both known contributors to endothelial injury and plaque development (167). Therefore, this response could be interpreted as a transient protective adaptation. However, this adaptation may not remain benign if triggered repeatedly over time. If voluntary jaw clenching induces uniform flow at an increased velocity frequently or for prolonged durations, the cumulative exposure to altered shear profiles, even if laminar, could still contribute to endothelial stress due to an increase in mechanical forces exerted on the endothelium surface (168). This highlights the importance of considering both the direction and duration of hemodynamic forces when evaluating their potential vascular impact.

Overall, it is important to acknowledge the hemodynamic consequences of frequent or sustained jaw activation and how it could lead to persistent shifts in flow distribution. Future studies should focus more specifically on the ECA to determine whether such flow alterations contribute to increased recirculation zones, altered shear stress profiles, or potential vascular remodeling. Understanding these changes could expand current models of carotid bifurcation dynamics and help uncover underappreciated vascular risks associated with chronic orofacial motor activity.

6.5 Facial Cooling

Our study used facial cooling as a method to decrease ECA blood flow by constricting the facial arteries to induce a non-metabolic vasoconstrictor response. Our results did not show changes in blood flow for any of the measured arteries (ECA, ICA, or CCA), nor in MCAv. This was unexpected since previous research has shown localized cooling of the face can effectively reduce facial blood flow and influence cerebral circulation through extracranial and intracranial interactions (16,104,169). Previous research has shown that cooling the facial

region with a 10°C stimulus can effectively reduce surface blood flow while minimizing the risk of excessive tissue hypoxia; however, this study used a water perfused mask that had consistently regulated water temperature inside the mask which was likely a more consistent cold stimulus than our study (114). While our study used a cold mask with a notably cooler temperature measured at 0.9 ± 1°C, it did not produce a substantial drop in facial temperature. The facial temperature decreased from 30.1°C to 24.1°C which is a modest difference of 6.0°C, therefore, the cold stimulus in our protocol did not trigger a strong enough vasoconstrictive response in the facial arteries to see changes in ICA or ECA blood flow. Although some degree of vasoconstriction likely occurred, it may not have been strong enough to influence downstream carotid artery blood flow or cause measurable changes in bulk flow distribution. Thus, the facial cooling protocol did not achieve the intended physiological effect.

Although we did not observe changes in blood flow during facial cooling, we surprisingly observed a decrease in ICA PI. Facial cooling is known to stimulate the trigeminal nerve and can lead to cerebral vasodilation through autonomic reflexes (170). One such reflex is the diving reflex, a physiological response typically characterized by bradycardia and peripheral vasoconstriction, which can be triggered by cold facial stimulation or breath holding (171). However, our data do not support full activation of the diving reflex, as heart rate remained unchanged and we did not assess peripheral vasoconstriction. It is possible that the decrease in PI reflects a mild or localized autonomic response, or was influenced by factors such as unintentional breath holding, although this cannot be confirmed from our data.

6.6 Clinical Significance in Dentistry

Bruxism is an orofacial disorder characterized by parafunctional muscle hyperactivity involving rhythmic and repetitive jaw activity such as clenching, grinding, tooth tapping, or cheek and lip biting (151,172–175). It can occur during the day (awake bruxism) or at night

(sleep bruxism) and can present in different patterns: phasic (brief, repeated contractions), tonic (sustained bursts lasting more than 2 seconds), or a combination of both (175,176). Up to 80–95% of the population experiences some form of bruxism (150), making it a significant clinical concern in the field of dentistry. The forceful nature of bruxism creates sustained pressure on the masseter muscle and surrounding vasculature, leading to hypertrophy of the masseter muscle, and increased occlusal forces causing symptoms such as mandibular pain, muscle fatigue, scalp tenderness, and headaches (177,178). Importantly, patients diagnosed with bruxism are at a higher risk of developing temporomandibular disorders (TMDs), a more severe, chronic condition affecting the masticatory muscles and temporomandibular joint (179,180). TMD is often considered a potential long-term complication of severe bruxism and is characterized by persistent pain, joint locking, clicking or popping sounds in the jaw, difficulty chewing or opening the mouth, and frequent headaches (181,182).

Despite bruxism having a high prevalence, the cause of it remains unclear. It has a multifactorial origin ranging from genetic and psychological factors to physiological and behavioral ones which makes it difficult to diagnose or treat definitively (151,183). While the dental consequences are well-established, including enamel wear, gum recession, and tooth damage and fractures (176,184), less is known about the potential vascular effects.

In our current study, we found that jaw clenching plays a role in modulating blood flow within the carotid system primarily increasing blood flow in the CCA, and ECA, increasing blood velocity and blood uniformity at the carotid bifurcation, as well as influencing MCAv. Of interest, the carotid bifurcation is a common site for atherosclerotic plaque development due to its unique geometry and complex flow patterns (22,64). As previously mentioned, while transient retrograde flow is considered a benign and physiologically normal feature of the carotid bifurcation, its clinical significance may shift in the context of habitual behaviors such as bruxism. Chronic exposure to altered shear environments, including persistent retrograde

flow, may promote maladaptive vascular remodeling, endothelial dysfunction, or early atherosclerotic changes (185). Bruxism has been linked to increased arterial stiffness in the aorta suggesting that chronic jaw muscle hyperactivity may have systemic vascular consequences beyond the masticatory system (186). Additionally, complex flow patterns at the carotid bifurcation are particularly concerning, since they contribute to endothelial dysfunction and play a key role in the development of atherosclerotic plaque (187). Although our study found that voluntary jaw clenching increased flow uniformity, it also increased velocity, which, if sustained chronically, could possibly impair endothelial function and exacerbate atherogenesis, particularly in individuals with pre-existing plaque. High WSS associated with high velocity is known to contribute to plaque destabilization and may lead to rupture, which can result in stroke (66,69). While the acute responses observed in our study were normal, repeated exposure to these hemodynamic outcomes may become a vascular stressor over time. Although this connection has not been established in the literature, it is something to make note of, and future research should further investigate. Further research is needed to investigate whether individuals with chronic jaw clenching behaviors exhibit early markers of carotid stiffening, intima-media thickening, or localized atherosclerotic change. If so, this would have major implications for how orofacial conditions like bruxism and TMD are viewed in the context of vascular health.

7.0 Limitations

One of the main limitations of this study was the absence of end-tidal CO_2 monitoring. A capnograph should have been used to track changes in the partial pressure of CO_2 in exhaled gases to identify subtle alterations in breathing patterns that may have influenced arterial CO_2 levels (90). Although participants were reminded to breath normally throughout the clenching periods, it is possible there may have been subtle changes in breathing during voluntary jaw clenching. Interpretating changes in MCAv assumes that MCA diameter remains consistent (97), which may not always hold true. Furthermore, continuous cardiovascular monitoring using finger plethysmography would have strengthened our interpretation by capturing beat-by-beat heart rate and blood pressure responses during voluntary jaw clenching.

Another limitation was the effectiveness of the facial cooling stimulus. It did not elicit the expected reduction in ECA blood flow, possibly due to insufficient cooling intensity or duration. Several adjustments could have improved the cooling protocol. For example, alternating between two chilled masks might have helped maintain a consistently low temperature. Once it became clear that facial temperature was not decreasing meaningfully, a second, pre-cooled mask could have been introduced, and the overall cooling period extended. Alternatively, applying the cold stimulus to the neck region, closer to the carotid bifurcation, may have provided a more direct thermal effect on the ECA (188).

While it would have been ideal to obtain direct measurements of blood flow in distal ECA branches such as the facial or maxillary artery to allow for more precise downstream assessment, time constraints limited our ability to include these additional measurements. Additionally, there was limited vector data of the carotid bifurcation, and it was difficult to standardize carotid orientations due to anatomical variability between participants.

Although the study was sex-balanced, we were underpowered to investigate sex-based differences in vascular responses to voluntary jaw clenching. This remains an important

direction for future research, particularly in light of emerging evidence suggesting a higher prevalence of bruxism among females (173). Additionally, while we did not include participants with dental related disorders, future research should consider populations with conditions such as bruxism or TMD, where altered facial muscle activity and chronic jaw tension may have a more pronounced impact on extracranial and intracranial vascular dynamics.

8.0 Conclusion

This study successfully used voluntary jaw clenching as a method to assess changes in blood flow in the carotid system. Our findings demonstrated that both isometric and dynamic clenching increased extracranial blood flow, while dynamic jaw clenching appeared to increase intracranial circulation to a greater extent. These results support the idea that the ECA plays an active regulatory role in upstream carotid flow dynamics, driven by localized changes in facial vascular resistance. Additionally, isometric jaw clenching was associated with increased velocity and flow uniformity, indicating an overall more uniform and laminar flow pattern at the carotid bifurcation. By demonstrating how facial muscle activity can directly influence blood flow patterns in the carotid system, this research offers a novel experimental model for investigating extracranial and intracranial hemodynamic redistribution. Such insights are particularly relevant to understanding vascular adaptations related to oromandibular activities and may shed light on pathophysiological mechanisms in orofacial conditions like bruxism and TMD. Future studies should aim to expand upon these findings by exploring blood flow responses in downstream facial artery branches and assessing these mechanisms in populations affected by bruxism or TMD. Investigating the interplay between facial vascular dynamics and cerebral circulation could reveal important links between oral health and cardiovascular function. Ultimately, bridging these gaps may lead to more integrative clinical approaches and a deeper understanding of oral-systemic vascular health.

References

1. Kambadakone A. Chapter 15 - Vascular Anatomy and Variants. In: Abbara S, Kalva SP, editors. Problem Solving in Cardiovascular Imaging [Internet]. Philadelphia (PA): W.B. Saunders; 2013 [cited 2024 Dec 14]. p. 248–66. Available from: https://www.sciencedirect.com/science/article/pii/B9781437727685000152

2. Michalinos A, Chatzimarkos M, Arkadopoulos N, Safioleas M, Troupis T. Anatomical Considerations on Surgical Anatomy of the Carotid Bifurcation. Anat Res Int. 2016;2016:6907472.

3. Jiang P, Chen Z, Hippe DS, Watase H, Sun B, Lin R, et al. Association Between Carotid Bifurcation Geometry and Atherosclerotic Plaque Vulnerability. Arterioscler Thromb Vasc Biol. 2020 May;40(5):1383–91.

4. Nichols WW, O'Rourke M, Edelman ER, Vlachopoulos C, editors. McDonald's Blood Flow in Arteries: Theoretical, Experimental and Clinical Principles. 7th ed. Boca Raton: CRC Press; 2022. 853 p.

5. Dhawan SS, Avati Nanjundappa RP, Branch JR, Taylor WR, Quyyumi AA, Jo H, et al. Shear stress and plaque development. Expert Rev Cardiovasc Ther. 2010 Apr;8(4):545–56.

6. Nicholls SC, Phillips DJ, Primozich JF, Lawrence RL, Kohler TR, Rudd TG, et al. Diagnostic significance of flow separation in the carotid bulb. Stroke. 1989 Feb;20(2):175–82.

7. Baun J. Emerging Technology: Ultrasound Vector Flow Imaging—A Novel Approach to Arterial Hemodynamic Quantification. J Diagn Med Sonogr. 2021 Nov 1;37(6):599–606.

8. Venkat P, Chopp M, Chen J. Chapter 12 - CBF–Metabolism Coupling. In: Caplan LR, Biller J, Leary MC, Lo EH, Thomas AJ, Yenari M, et al., editors. Primer on Cerebrovascular Diseases (Second Edition) [Internet]. San Diego: Academic Press; 2017 [cited 2025 Jan 22]. p. 67–70. Available from: https://www.sciencedirect.com/science/article/pii/B9780128030585000126

9. Ruland S, Aiyagari V. Cerebral Autoregulation and Blood Pressure Lowering. Hypertension. 2007 May;49(5):977–8.

10. Ogoh S, Washio T, Paton JFR, Fisher JP, Petersen LG. Gravitational effects on intracranial pressure and blood flow regulation in young men: a potential shunting role for the external carotid artery. J Appl Physiol. 2020 Oct;129(4):901–8.

11. Garcia FA, Spavieri DL, Linninger A. Cerebral hemodynamics: a mathematical model including autoregulation, baroreflex and extracranial peripheral circulation [Internet]. bioRxiv; 2021 [cited 2025 Jan 22]. p. 2021.06.11.448061. Available from: https://www.biorxiv.org/content/10.1101/2021.06.11.448061v3

12. Kaszczewski P, Elwertowski M, Leszczyński J, Ostrowski T, Kaszczewska J, Gałązka Z. Intracranial Flow Volume Estimation in Patients with Internal Carotid Artery Occlusion. Diagnostics. 2022 Mar;12(3):766.

13. Fearn SJ, Picton AJ, Mortimer AJ, Parry AD, McCollum CN. The contribution of the external carotid artery to cerebral perfusion in carotid disease. J Vasc Surg. 2000 May 1;31(5):989–93.

14. Ogoh S, Sugawara J, Shibata S. Does Cardiac Function Affect Cerebral Blood Flow Regulation? J Clin Med. 2022 Oct 13;11(20):6043.

15. Sato K, Ogoh S, Hirasawa A, Oue A, Sadamoto T. The distribution of blood flow in the carotid and vertebral arteries during dynamic exercise in humans. J Physiol. 2011 June 1;589(Pt 11):2847–56.

16. Miyazawa T, Horiuchi M, Ichikawa D, Subudhi AW, Sugawara J, Ogoh S. Face cooling with mist water increases cerebral blood flow during exercise: effect of changes in facial skin blood flow. Front Physiol. 2012;3:308.

17. Ogoh S, Lericollais R, Hirasawa A, Sakai S, Normand H, Bailey DM. Regional redistribution of blood flow in the external and internal carotid arteries during acute hypotension. Am J Physiol-Regul Integr Comp Physiol. 2014 May 15;306(10):R747–51.

18. Bond JD, Zheng F, Wang Q, Zhang M. The carotid sheath: Anatomy and clinical considerations. World Neurosurg X. 2023 Jan 24;18:100158.

19. Kaufman JA, Nesbit GM. CHAPTER 5 - Carotid and Vertebral Arteries. In: Kaufman JA, Lee MJ, editors. Vascular and Interventional Radiology [Internet]. Philadelphia: W.B. Saunders; 2004 [cited 2024 Dec 14]. p. 119–41. (The Requisites). Available from: https://www.sciencedirect.com/science/article/pii/B9780815143697500135

20. Gasser TC, Ogden RW, Holzapfel GA. Hyperelastic modelling of arterial layers with distributed collagen fibre orientations. J R Soc Interface. 2006 Feb 22;3(6):15–35.

21. Labrosse M, editor. Cardiovascular Mechanics. Boca Raton: CRC Press; 2018. 400 p.

22. Zarins CK, Giddens DP, Bharadvaj BK, Sottiurai VS, Mabon RF, Glagov S. Carotid bifurcation atherosclerosis. Quantitative correlation of plaque localization with flow velocity profiles and wall shear stress. Circ Res. 1983 Oct;53(4):502–14.

23. Ismail A, Ravipati S, Gonzalez-Hernandez D, Mahmood H, Imran A, Munoz EJ, et al. Carotid Artery Stenosis: A Look Into the Diagnostic and Management Strategies, and Related Complications. Cureus. 15(5):e38794.

24. Schulz UGR, Rothwell PM. Major Variation in Carotid Bifurcation Anatomy. Stroke. 2001 Nov;32(11):2522–9.

25. Arumugam S, Subbiah NK. A Cadaveric Study on the Course of the Cervical Segment of the Internal Carotid Artery and Its Variations. Cureus. 12(4):e7663.

26. Saqr KM, Tupin S, Rashad S, Endo T, Niizuma K, Tominaga T, et al. Physiologic blood flow is turbulent. Sci Rep. 2020 Sept 23;10(1):15492.

27. Yellin EL. Laminar-turbulent transition process in pulsatile flow. Circ Res. 1966 Oct;19(4):791–804.

28. Guo B, Ghalambor A. Chapter 11 - Transportation. In: Guo B, Ghalambor A, editors. Natural Gas Engineering Handbook (Second Edition) [Internet]. Gulf Publishing Company; 2005 [cited 2024 Dec 23]. p. 219–62. Available from: https://www.sciencedirect.com/science/article/pii/B9781933762418500186

29. Bark DL, Vital EF, Oury C, Lam WA, Gardiner EE. Recommendations for defining disturbed flow as laminar, transitional, or turbulent in assays of hemostasis and thrombosis: communication from the ISTH SSC Subcommittee on Biorheology. J Thromb Haemost [Internet]. 2024 Oct 10 [cited 2024 Dec 23]; Available from: https://www.sciencedirect.com/science/article/pii/S1538783624005749

30. Owen CA, Roberts M. Arterial Vascular Hemodynamics. J Diagn Med Sonogr. 2007 May 1;23(3):129–40.

31. Goddi A, Bortolotto C, Fiorina I, Raciti MV, Fanizza M, Turpini E, et al. High-frame rate vector flow imaging of the carotid bifurcation. Insights Imaging. 2017 May 12;8(3):319–28.

32. Ardakani SSJ, Jafarnejad M, Firoozabadi B, Saidi MS. Investigation of Wall Shear Stress Related Factors in Realistic Carotid Bifurcation Geometries and Di erent Flow Conditions.

33. Goubergrits L, Affeld K, Fernandez-Britto J, Falcon L. Geometry of the human common carotid artery. A vessel cast study of 86 specimens. Pathol Res Pract. 2002;198(8):543–51.

34. Phan TG, Beare RJ, Jolley D, Das G, Ren M, Wong K, et al. Carotid Artery Anatomy and Geometry as Risk Factors for Carotid Atherosclerotic Disease. Stroke. 2012 June;43(6):1596–601.

35. Nguyen KT, Clark CD, Chancellor TJ, Papavassiliou DV. Carotid geometry effects on blood flow and on risk for vascular disease. J Biomech. 2008;41(1):11–9.

36. Vijaywargiya M, Deopujari R, Athavale SA. Anatomical study of petrous and cavernous parts of internal carotid artery. Anat Cell Biol. 2017 Sept;50(3):163–70.

37. Wolman DN, Moraff AM, Heit JJ. Anatomy of the Intracranial Arteries: The Internal Carotid Artery. Neuroimaging Clin N Am. 2022 Aug 1;32(3):603–15.

38. Charlick M, Das JM. Anatomy, Head and Neck: Internal Carotid Arteries. In: StatPearls [Internet]. Treasure Island (FL): StatPearls Publishing; 2024 [cited 2024 Dec 15]. Available from: http://www.ncbi.nlm.nih.gov/books/NBK556061/

39. Lee W. General principles of carotid Doppler ultrasonography. Ultrasonography. 2014 Jan;33(1):11–7.

40. Gosling RG, King DH. The Role of Measurement in Peripheral Vascular Surgery: Arterial Assessment by Doppler-shift Ultrasound. Proc R Soc Med. 1974 June 1;67(6P1):447–9.

41. Wielicka M, Neubauer-Geryk J, Kozera G, Bieniaszewski L. Clinical application of pulsatility index. Med Res J. 2020;5(3):201–10.

42. de Riva N, Budohoski KP, Smielewski P, Kasprowicz M, Zweifel C, Steiner LA, et al. Transcranial Doppler Pulsatility Index: What it is and What it Isn't. Neurocrit Care. 2012 Aug 1;17(1):58–66.

43. van Tuijl RJ, Ruigrok YM, Velthuis BK, van der Schaaf IC, Rinkel GJE, Zwanenburg JJM. Velocity Pulsatility and Arterial Distensibility Along the Internal Carotid Artery. J Am Heart Assoc Cardiovasc Cerebrovasc Dis. 2020 Aug 12;9(16):e016883.

44. James NL, Milijasevic Z, Ujhazy A, Edwards G, Jermyn K, Mynard JP, et al. The common carotid artery provides significant pressure wave dampening in the young adult sheep. IJC Heart Vasc. 2019 June 1;23:100343.

45. Motomiya M, Karino T. Flow patterns in the human carotid artery bifurcation. Stroke. 1984;15(1):50–6.

46. Middleton WD, Foley WD, Lawson TL. Flow reversal in the normal carotid bifurcation: color Doppler flow imaging analysis. Radiology. 1988 Apr;167(1):207–10.

47. Cecchi E, Giglioli C, Valente S, Lazzeri C, Gensini GF, Abbate R, et al. Role of hemodynamic shear stress in cardiovascular disease. Atherosclerosis. 2011 Feb;214(2):249–56.

48. Younis HF, Kaazempur-Mofrad MR, Chan RC, Isasi AG, Hinton DP, Chau AH, et al. Hemodynamics and wall mechanics in human carotid bifurcation and its consequences for atherogenesis: investigation of inter-individual variation. Biomech Model Mechanobiol. 2004 Sept;3(1):17–32.

49. Khanal L, Koirala S, Shah S, Pandeya A. Bilateral anatomical variation in branching pattern of external carotid artery in a male cadaver: A case report. Russ Open Med J. 2014 June 24;3(2):0203.

50. Hasan TF, Akinduro OO, Haranhalli N, Tawk RG. Chapter 3 - Neurovascular Anatomy in Relation to Intracranial Neoplasms. In: Chaichana K, Quiñones-Hinojosa A, editors. Comprehensive Overview of Modern Surgical Approaches to Intrinsic Brain Tumors [Internet]. Academic Press; 2019 [cited 2024 Dec 16]. p. 37–51. Available from: https://www.sciencedirect.com/science/article/pii/B9780128117835000033

51. Devadas D, Pillay M, Sukumaran TT. A cadaveric study on variations in branching pattern of external carotid artery. Anat Cell Biol. 2018 Dec;51(4):225–31.

52. Miceli G, Tuttolomondo A, Velardo M, Bencivinni F, Poma S, Pinto A. “The importance of being external”: review of the literature of the rare phenomenon of common carotid occlusion with bulb reverse-crossed stenosis and external collaterals activation. Is still correct speaking about carotid steal? J Ultrasound. 2022 Jan 15;25(3):435–42.

53. Reid DB, Irshad K, Miller S, Reid AW, Reid W, Diethrich EB. Endovascular significance of the external carotid artery in the treatment of cerebrovascular insufficiency. J Endovasc Ther Off J Int Soc Endovasc Spec. 2004 Dec;11(6):727–33.

54. Meyer S, Wilde L, Wolf F, Liman J, Bähr M, Maier IL. Doppler flow morphology characteristics of epiaortic arteries in aortic valve pathologies: a retrospective study on a cohort of patients with ischemic stroke. Ultrasound J. 2023 June 7;15(1):29.

55. Meyer P, Pelz JO. Blood flow reversal from the external into the internal carotid artery—New insights into the hemodynamics at the carotid bifurcation. Brain Behav. 2018 Oct 12;8(11):e01139.

56. Schuierer G, Huk WJ. Diagnostic significance of flow separation within the carotid bifurcation demonstrated by digital subtraction angiography. Stroke. 1990 Dec;21(12):1674–9.

57. Rajani RR. How much should we know about the external carotid artery? J Vasc Surg. 2020 Sept;72(3):958.

58. Venna N, Goldman R, Tilak S, Sabin TD. Temporal arteritis-like presentation of carotid atherosclerosis. Stroke. 1986;17(2):325–7.

59. Weyand CM, Goronzy JJ. Immunology of Giant Cell Arteritis. Circ Res. 2023 Jan 20;132(2):238–50.

60. Boysson H de, Liozon E, Larivière D, Samson M, Parienti JJ, Boutemy J, et al. Giant Cell Arteritis–related Stroke: A Retrospective Multicenter Case-control Study. J Rheumatol. 2017 Mar 1;44(3):297–303.

61. Fayyaz B. Case report: giant cell arteritis in a patient with carotid atherosclerosis – a diagnostic dilemma. J Community Hosp Intern Med Perspect. 2018 June 12;8(3):134–7.

62. Norman JE de B. Facial pain and vascular disease: Some clinical observations. Br J Oral Surg. 1970 Jan 1;8(2):138–44.

63. Peral-Cagigal B, Pérez-Villar Á, Redondo-González LM, García-Sierra C, Morante-Silva M, Madrigal-Rubiales B, et al. Temporal headache and jaw claudication may be the key for the diagnosis of giant cell arteritis. Med Oral Patol Oral Cir Bucal. 2018 May;23(3):e290–4.

64. Bir SC, Kelley RE. Carotid atherosclerotic disease: A systematic review of pathogenesis and management. Brain Circ. 2022 Sept 21;8(3):127–36.

65. Moerman AM, Korteland S, Dilba K, van Gaalen K, Poot DHJ, van Der Lugt A, et al. The Correlation Between Wall Shear Stress and Plaque Composition in Advanced Human

Carotid Atherosclerosis. Front Bioeng Biotechnol [Internet]. 2022 Jan 28 [cited 2025 Aug 12];9. Available from: https://www.frontiersin.org/journals/bioengineering-and-biotechnology/articles/10.3389/fbioe.2021.828577/full

66. Zhou M, Yu Y, Chen R, Liu X, Hu Y, Ma Z, et al. Wall shear stress and its role in atherosclerosis. Front Cardiovasc Med [Internet]. 2023 Apr 3 [cited 2025 Aug 12];10. Available from: https://www.frontiersin.org/journals/cardiovascular-medicine/articles/10.3389/fcvm.2023.1083547/full

67. Malek AM, Alper SL, Izumo S. Hemodynamic Shear Stress and Its Role in Atherosclerosis. JAMA. 1999 Dec 1;282(21):2035–42.

68. Giannoglou G, Antoniadis A, Koskinas K, Chatzizisis Y. Flow and atherosclerosis in coronary bifurcations. EuroIntervention. 2010 Dec;6(J):J16–23.

69. Stefanadis C, Antoniou C, Tsiachris D, Pietri P. Coronary Atherosclerotic Vulnerable Plaque: Current Perspectives. J Am Heart Assoc. 2017 Mar 17;6(3):e005543.

70. Bonati LH, Kakkos S, Berkefeld J, de Borst GJ, Bulbulia R, Halliday A, et al. European Stroke Organisation guideline on endarterectomy and stenting for carotid artery stenosis. Eur Stroke J. 2021 June 1;6(2):I–XLVII.

71. Treat-Jacobson DJ, Rich K, DeVeaux T, Fitzgerald K, Flood A, Gilpin V, et al. Society for Vascular Nursing clinical practice guideline (CPG) for carotid artery stenting. J Vasc Nurs. 2013 Mar 1;31(1):32–55.

72. Lee SW, Antiga L, Spence JD, Steinman DA. Geometry of the carotid bifurcation predicts its exposure to disturbed flow. Stroke. 2008 Aug;39(8):2341–7.

73. Schulz UGR, Rothwell PM. Sex Differences in Carotid Bifurcation Anatomy and the Distribution of Atherosclerotic Plaque. Stroke. 2001 July;32(7):1525–31.

74. Iemolo F, Martiniuk A, Steinman DA, Spence JD. Sex Differences in Carotid Plaque and Stenosis. Stroke. 2004 Feb;35(2):477–81.

75. Claassen JAHR, Thijssen DHJ, Panerai RB, Faraci FM. Regulation of cerebral blood flow in humans: physiology and clinical implications of autoregulation. Physiol Rev. 2021 Oct;101(4):1487–559.

76. Brassard P, Labrecque L, Smirl JD, Tymko MM, Caldwell HG, Hoiland RL, et al. Losing the dogmatic view of cerebral autoregulation. Physiol Rep. 2021 Aug;9(15):e14982.

77. Cole WC, Welsh DG. Role of myosin light chain kinase and myosin light chain phosphatase in the resistance arterial myogenic response to intravascular pressure. Arch Biochem Biophys. 2011 June 15;510(2):160–73.

78. Williams LR, Leggett RW. Reference values for resting blood flow to organs of man. Clin Phys Physiol Meas Off J Hosp Phys Assoc Dtsch Ges Med Phys Eur Fed Organ Med Phys. 1989 Aug;10(3):187–217.

79. Meng L, Hou W, Chui J, Han R, Gelb AW. Cardiac Output and Cerebral Blood Flow: The Integrated Regulation of Brain Perfusion in Adult Humans. Anesthesiology. 2015 Nov;123(5):1198–208.

80. Ogoh S, Brothers RM, Barnes Q, Eubank WL, Hawkins MN, Purkayastha S, et al. The effect of changes in cardiac output on middle cerebral artery mean blood velocity at rest and during exercise. J Physiol. 2005 Dec 1;569(Pt 2):697–704.

81. Touzani O, MacKenzie ET. CHAPTER 41 - ANATOMY AND PHYSIOLOGY OF CEREBRAL AND SPINAL CORD CIRCULATION. In: Schapira AHV, Byrne E, DiMauro S, Frackowiak RSJ, Johnson RT, Mizuno Y, et al., editors. Neurology and Clinical Neuroscience [Internet]. Philadelphia: Mosby; 2007 [cited 2024 Dec 16]. p. 540–9. Available from: https://www.sciencedirect.com/science/article/pii/B9780323033541500456

82. Vrselja Z, Brkic H, Mrdenovic S, Radic R, Curic G. Function of circle of Willis. J Cereb Blood Flow Metab Off J Int Soc Cereb Blood Flow Metab. 2014 Apr;34(4):578–84.

83. Nagata K, Yamazaki T, Takano D, Maeda T, Fujimaki Y, Nakase T, et al. Cerebral circulation in aging. Ageing Res Rev. 2016 Sept 1;30:49–60.

84. Navarro-Orozco D, Sánchez-Manso JC. Neuroanatomy, Middle Cerebral Artery. In: StatPearls [Internet]. Treasure Island (FL): StatPearls Publishing; 2024 [cited 2024 Dec 16]. Available from: http://www.ncbi.nlm.nih.gov/books/NBK526002/

85. Jarrett CL, Shields KL, Broxterman RM, Hydren JR, Park SH, Gifford JR, et al. Imaging transcranial Doppler ultrasound to measure middle cerebral artery blood flow: the importance of measuring vessel diameter. Am J Physiol - Regul Integr Comp Physiol. 2020 July 1;319(1):R33–42.

86. Stock KW, Wetzel SG, Lyrer PA, Radü EW. Quantification of blood flow in the middle cerebral artery with phase-contrast MR imaging. Eur Radiol. 2000 Oct;10(11):1795–800.

87. Markwalder TM, Grolimund P, Seiler RW, Roth F, Aaslid R. Dependency of blood flow velocity in the middle cerebral artery on end-tidal carbon dioxide partial pressure--a transcranial ultrasound Doppler study. J Cereb Blood Flow Metab Off J Int Soc Cereb Blood Flow Metab. 1984 Sept;4(3):368–72.

88. Moraine JJ, Lamotte M, Berré J, Niset G, Leduc A, Naeije R. Relationship of middle cerebral artery blood flow velocity to intensity during dynamic exercise in normal subjects. Eur J Appl Physiol. 1993;67(1):35–8.

89. Giller CA, Giller AM, Cooper CR, Hatab MR. Evaluation of the cerebral hemodynamic response to rhythmic handgrip. J Appl Physiol Bethesda Md 1985. 2000 June;88(6):2205–13.

90. Lam T, Nagappa M, Wong J, Singh M, Wong D, Chung F. Continuous Pulse Oximetry and Capnography Monitoring for Postoperative Respiratory Depression and

Adverse Events: A Systematic Review and Meta-analysis. Anesth Analg. 2017 Dec;125(6):2019.

91. Charkoudian N. Skin Blood Flow in Adult Human Thermoregulation: How It Works, When It Does Not, and Why. Mayo Clin Proc. 2003 May 1;78(5):603–12.

92. Nybo L, Møller K, Volianitis S, Nielsen B, Secher NH. Effects of hyperthermia on cerebral blood flow and metabolism during prolonged exercise in humans. J Appl Physiol Bethesda Md 1985. 2002 July;93(1):58–64.

93. Nybo L, Nielsen B. Middle cerebral artery blood velocity is reduced with hyperthermia during prolonged exercise in humans. J Physiol. 2001 July 1;534(Pt 1):279–86.

94. Ainslie PN, Duffin J. Integration of cerebrovascular CO2 reactivity and chemoreflex control of breathing: mechanisms of regulation, measurement, and interpretation. Am J Physiol Regul Integr Comp Physiol. 2009 May;296(5):R1473-1495.

95. Rasmussen P, Stie H, Nielsen B, Nybo L. Enhanced cerebral CO2 reactivity during strenuous exercise in man. Eur J Appl Physiol. 2006 Feb;96(3):299–304.

96. Ogoh S, Sato K, Okazaki K, Miyamoto T, Hirasawa A, Shibasaki M. Hyperthermia modulates regional differences in cerebral blood flow to changes in CO2. J Appl Physiol. 2014 July;117(1):46–52.

97. Hasegawa Y, Ono T, Hori K, Nokubi T. Influence of human jaw movement on cerebral blood flow. J Dent Res. 2007 Jan;86(1):64–8.

98. Janssens M a. P, Van Thielen THJ, Van Veer HGL. Jaw claudication as a result of carotid artery disease. Acta Chir Belg. 2008;108(4):438–40.

99. Oglat AA, Matjafri MZ, Suardi N, Oqlat MA, Abdelrahman MA, Oqlat AA. A Review of Medical Doppler Ultrasonography of Blood Flow in General and Especially in Common Carotid Artery. J Med Ultrasound. 2018;26(1):3–13.

100. Qiu Y, Dong Y, Mao F, Zhang Q, Yang D, Chen K, et al. High-Frame Rate Vector Flow Imaging Technique: Initial Application in Evaluating the Hemodynamic Changes of Carotid Stenosis Caused by Atherosclerosis. Front Cardiovasc Med. 2021 Mar 8;8:617391.

101. Haniel J, Yiu BYS, Chee AJY, Huebner R, Yu ACH. Efficacy of ultrasound vector flow imaging in tracking omnidirectional pulsatile flow. Med Phys. 2023 Mar;50(3):1699–714.

102. Faul F, Erdfelder E, Buchner A, Lang AG. Statistical power analyses using G*Power 3.1: Tests for correlation and regression analyses. Behav Res Methods. 2009 Nov;41(4):1149–60.

103. WebPlotDigitizer - Copyright 2010-2024 Ankit Rohatgi [Internet]. [cited 2025 July 25]. Available from: https://apps.automeris.io/wpd4/

104. Nakata H, Namba M, Kakigi R, Shibasaki M. Effects of face/head and whole body cooling during passive heat stress on human somatosensory processing. Am J Physiol-Regul Integr Comp Physiol. 2017 June;312(6):R996–1003.

105. Ogoh S, Sato K, Hirasawa A, Sadamoto T. The effect of muscle metaboreflex on the distribution of blood flow in cerebral arteries during isometric exercise. J Physiol Sci. 2019 Mar;69(2):375–85.

106. Lin SK, Chang YJ, Ryu SJ, Chu NS. Cerebral Hemodynamic Responses to Betel Chewing: A Doppler Study. Clin Neuropharmacol. 2002 Oct;25(5):244.

107. Papaharilaou Y, Aristokleous N, Seimenis I, Khozeymeh MI, Georgiou GC, Brott BC, et al. Effect of head posture on the healthy human carotid bifurcation hemodynamics. Med Biol Eng Comput. 2013 Feb;51(1–2):207–18.

108. Glor FP, Ariff B, Hughes AD, Verdonck PR, Barratt DC, Augst AD, et al. Influence of head position on carotid hemodynamics in young adults. Am J Physiol Heart Circ Physiol. 2004 Oct;287(4):H1670-1681.

109. Favre ME, Lim V, Falvo MJ, Serrador JM. Cerebrovascular reactivity and cerebral autoregulation are improved in the supine posture compared to upright in healthy men and women. Mogi M, editor. PLOS ONE. 2020 Mar 2;15(3):e0229049.

110. Rasmussen OC, Bonde-Petersen F, Christensen LV, Møller E. Blood flow in human mandibular elevators at rest and during controlled biting. Arch Oral Biol. 1977 Jan 1;22(8):539–43.

111. Kim YJ, Kuboki T, Tsukiyama Y, Koyano K, Clark GT. Haemodynamic changes in human masseter and temporalis muscles induced by different levels of isometric contraction. Arch Oral Biol. 1999 Aug 1;44(8):641–50.

112. Otomo N NA. Magnitude of Bite Force that is Interpreted as Clenching in Patients with Temporomandibular Disorders: A Pilot Study. Dentistry [Internet]. 2014 [cited 2025 Jan 12];s2(01). Available from: https://www.omicsonline.org/open-access/magnitude-of-bite-force-that-is-interpreted-as-clenching-in-patients-with-temporomandibular-disorders-a-pilot-study-2161-1122.S2-004.php?aid=28693

113. 3 Second Interval Timer [Internet]. 2024 [cited 2025 May 30]. Available from: https://www.youtube.com/watch?v=fTUZw5NasUI

114. Peters F, Heussen N, Herbstmann J, Möhlhenrich SC, Bock A, Kniha K, et al. Evaluation of the optimal cooling temperature for the face measured by the tissue perfusion during hilotherapy using laser Doppler spectrophotometry. Sci Rep. 2021 May 7;11(1):9805.

115. Innobyte [Internet]. [cited 2025 May 30]. User Guide - Innobyte | Kube Innovation. Available from: https://www.kubeinnovation.com/documentation

116. Koolstra JH. Dynamics of the Human Masticatory System. Crit Rev Oral Biol Med. 2002 July 1;13(4):366–76.

117. Nishi SE, Rahman NA, Basri R, Alam MK, Noor NFM, Zainal SA, et al. Surface Electromyography (sEMG) Activity of Masticatory Muscle (Masseter and Temporalis) with Three Different Types of Orthodontic Bracket. BioMed Res Int. 2021 Apr 21;2021:6642254.

118. Au JS, Yiu BYS, So H, Chee AJY, Greaves DK, Hughson RL, et al. Ultrasound vector projectile imaging for detection of altered carotid bifurcation hemodynamics during reductions in cardiac output. Med Phys. 2020;47(2):431–40.

119. Cohen JN, Jasiak JN, Nahas H, Yu ACH, Au JS. Multidirectional blood flow in the femoral artery via vector flow imaging: Doppler ultrasound imaging insights. Am J Physiol-Heart Circ Physiol. 2024 Dec;327(6):H1467–73.

120. Yiu BYS, Walczak M, Lewandowski M, Yu ACH. Live Ultrasound Color-Encoded Speckle Imaging Platform for Real-Time Complex Flow Visualization In Vivo. IEEE Trans Ultrason Ferroelectr Freq Control. 2019 Apr;66(4):656–68.

121. Yiu BYS, Yu ACH. Least-Squares Multi-Angle Doppler Estimators for Plane-Wave Vector Flow Imaging. IEEE Trans Ultrason Ferroelectr Freq Control. 2016 Nov;63(11):1733–44.

122. Cohen JN, Hedge ET, Greaves DK, Robertson AD, Nahas H, Yu ACH, et al. Characterization of internal jugular vein region-specific distension and flow patterns during progressive volume shifting. J Appl Physiol. 2024 July;137(1):32–41.

123. Yiu BYS, Lai SSM, Yu ACH. Vector Projectile Imaging: Time-Resolved Dynamic Visualization of Complex Flow Patterns. Ultrasound Med Biol. 2014 Sept;40(9):2295–309.

124. Pedersen MM, Pihl MJ, Haugaard P, Hansen KL, Lange T, Lönn L, et al. Novel Flow Quantification of the Carotid Bulb and the Common Carotid Artery with Vector Flow Ultrasound. Ultrasound Med Biol. 2014 Nov 1;40(11):2700–6.

125. Bouzat P, Oddo M, Payen JF. Transcranial Doppler after traumatic brain injury: is there a role? Curr Opin Crit Care. 2014 Apr;20(2):153–60.

126. Coolbaugh CL, Bush EC, Caskey CF, Damon BM, Towse TF. FloWave.US: validated, open-source, and flexible software for ultrasound blood flow analysis. J Appl Physiol. 2016 Oct;121(4):849–57.

127. Cohen JN, Sole RT, Zafiris E, Au JS. Efficacy of a hands-free vascular ultrasound probe holder in active and inactive limbs during cycling exercise. J Appl Physiol. 2025 Feb;138(2):389–96.

128. van Hespen KM, Kuijf HJ, Hendrikse J, Luijten PR, Zwanenburg JJM. Blood Flow Velocity Pulsatility and Arterial Diameter Pulsatility Measurements of the Intracranial Arteries Using 4D PC-MRI. Neuroinformatics. 2022;20(2):317–26.

129. Srikumar S, Debnath J, Ravikumar R, Bandhu HC, Maurya VK. Doppler indices of the umbilical and fetal middle cerebral artery at 18–40 weeks of normal gestation: A pilot study. Med J Armed Forces India. 2017 July;73(3):232–41.

130. Kallenberg LA, Hermens HJ. Behaviour of motor unit action potential rate, estimated from surface EMG, as a measure of muscle activation level. J NeuroEngineering Rehabil. 2006 July 17;3:15.

131. Fukuda TY, Echeimberg JO, Pompeu JE, Lucareli PRG, Garbelotti S, Gimenes RO, et al. Root Mean Square value of the electromyographic signal in the isometric torque of the quadriceps, hamstrings and brachial biceps muscles in female subjects. J Appl Res. 2010 Mar 1;10(1):32–40.

132. Methodological Differences in the Interpretation of Fatigue Data from Repeated Maximal Effort Knee Extensions. Open Sports Sci J. 2017 Jan 1;10:37–51.

133. R: The R Project for Statistical Computing [Internet]. [cited 2025 Apr 22]. Available from: https://www.r-project.org/

134. Gliemann L, Vestergaard Hansen C, Rytter N, Hellsten Y. Regulation of skeletal muscle blood flow during exercise. Curr Opin Physiol. 2019 Aug 1;10:146–55.

135. Korthuis RJ. Exercise Hyperemia and Regulation of Tissue Oxygenation During Muscular Activity. In: Skeletal Muscle Circulation [Internet]. Morgan & Claypool Life Sciences; 2011 [cited 2025 July 16]. Available from: https://www.ncbi.nlm.nih.gov/books/NBK57139/

136. Pomella N, Wilhelm EN, Kolyva C, González-Alonso J, Rakobowchuk M, Khir AW. Noninvasive assessment of the common carotid artery hemodynamics with increasing exercise work rate using wave intensity analysis. Am J Physiol - Heart Circ Physiol. 2018 Aug 1;315(2):H233–41.

137. Korthuis RJ. Regulation of Vascular Tone in Skeletal Muscle. In: Skeletal Muscle Circulation [Internet]. Morgan & Claypool Life Sciences; 2011 [cited 2025 July 17]. Available from: https://www.ncbi.nlm.nih.gov/books/NBK57142/

138. Hellstrom G, Fischer-Colbrie W, Wahlgren NG, Jogestrand T. Carotid artery blood flow and middle cerebral artery blood flow velocity during physical exercise. J Appl Physiol. 1996 July;81(1):413–8.

139. Hayashi N, Kashima H, Ikemura T. Facial Blood Flow Responses to Dynamic Exercise. Int J Sports Med. 2021 Mar;42(3):241–5.

140. Curtis DA, Gansky SA, Plesh O. Deep and superficial masseter muscle blood flow in women. J Prosthodont Off J Am Coll Prosthodont. 2012 Aug 1;21(6):472–7.

141. Nakamura Y, Torisu T, Noguchi K, Fujii H. Changes in masseter muscle blood flow during voluntary isometric contraction in humans. J Oral Rehabil. 2005;32(8):545–51.

142. Monteiro AA, Kopp S. Estimation of blood flow by 133Xe clearance in human masseter muscle during rest, endurance of isometric contraction, and recovery. Arch Oral Biol. 1988 Jan 1;33(8):561–5.

143. Rasmussen OC, Bonde-Petersen F, Christensen LV, Møller E. Blood flow in human mandibular elevators at rest and during controlled biting. Arch Oral Biol. 1977;22(8–9):539–43.

144. Ogoh S, Fisher JP, Purkayastha S, Dawson EA, Fadel PJ, White MJ, et al. Regulation of middle cerebral artery blood velocity during recovery from dynamic exercise in humans. J Appl Physiol. 2007 Feb;102(2):713–21.

145. Washio T, Suzuki K, Yamagata T, Ando S, Ogoh S. Effect Of Isometric Handgrip Exercise On Hypercapnia-induced Shear-mediated Dilation In The Internal Carotid Artery: 2448 Board #112 May 31 11:00 AM - 12:30 PM. Med Sci Sports Exerc. 2019 June;51(6S):671.

146. Hasegawa Y, Sakagami J, Ono T, Hori K, Zhang M, Maeda Y. Circulatory response and autonomic nervous activity during gum chewing. Eur J Oral Sci. 2009;117(4):470–3.

147. Momose T, Nishikawa J, Watanabe T, Sasaki Y, Senda M, Kubota K, et al. Effect of mastication on regional cerebral blood flow in humans examined by positron-emission tomography with 15O-labelled water and magnetic resonance imaging. Arch Oral Biol. 1997 Jan 1;42(1):57–61.

148. Evans DH, Barrie WW, Asher MJ, Bentley S, Bell PR. The relationship between ultrasonic pulsatility index and proximal arterial stenosis in a canine model. Circ Res. 1980 Apr;46(4):470–5.

149. Kristiansson H, Nissborg E, Bartek JJ, Andresen M, Reinstrup P, Romner B. Measuring Elevated Intracranial Pressure through Noninvasive Methods: A Review of the Literature. J Neurosurg Anesthesiol. 2013 Oct;25(4):372.

150. Jorgensen LG, Perko G, Secher NH. Regional cerebral artery mean flow velocity and blood flow during dynamic exercise in humans. J Appl Physiol. 1992 Nov;73(5):1825–30.

151. Uchima Koecklin KH, Aliaga-Del Castillo A, Li P. The neural substrates of bruxism: current knowledge and clinical implications. Front Neurol [Internet]. 2024 Oct 1 [cited 2025 Aug 1];15. Available from: https://www.frontiersin.org/journals/neurology/articles/10.3389/fneur.2024.1451183/full

152. Svensson P, De Laat A, Graven-Nielsen T, Arendt-Nielsen L, Macaluso GM. Effect of clenching levels on heteronymous H-reflex in human temporalis muscle. Exp Brain Res. 1999 June 1;126(4):467–72.

153. Watson C, Walshaw D, McMillan AS. Effect of motor tasks on the cortical topography of the human masseter muscle. Arch Oral Biol. 2000 Sept 1;45(9):767–73.

154. Iida T, Komiyama O, Obara R, Baad-Hansen L, Kawara M, Svensson P. Repeated clenching causes plasticity in corticomotor control of jaw muscles. Eur J Oral Sci. 2014;122(1):42–8.

155. Venkatesh IH, Shubha HV, Karthik N, RaviShankar S. A Study of Reversal of Diastolic Blood Flow in the Middle Cerebral Artery Using Doppler Ultrasound in the Prognostication in Sick Neonates. J Clin Neonatol. 2020 Mar;9(1):52.

156. Jiang ZL, Yamaguchi H, Takahashi A, Tanabe S, Utsuyama N, Ikehara T, et al. Blood flow velocity in the common carotid artery in humans during graded exercise on a treadmill. Eur J Appl Physiol. 1995 Mar 1;70(3):234–9.

157. Hirasawa A, Sato K, Yoneya M, Sadamoto T, Bailey DM, Ogoh S. Heterogeneous Regulation of Brain Blood Flow during Low-Intensity Resistance Exercise. Med Sci Sports Exerc. 2016 Sept;48(9):1829–34.

158. Donnelly J, Budohoski KP, Smielewski P, Czosnyka M. Regulation of the cerebral circulation: bedside assessment and clinical implications. Crit Care. 2016;20:129.

159. Ogoh S, Moralez G, Washio T, Sarma S, Hieda M, Romero SA, et al. Effect of increases in cardiac contractility on cerebral blood flow in humans. Am J Physiol - Heart Circ Physiol. 2017 Dec 1;313(6):H1155–61.

160. Rani TR, Shibli AA, Siraj M, Srimal W, Bakri NZSA, Radhika TSL. ML-Based Approach to Predict Carotid Arterial Blood Flow Dynamics. Contemp Math. 2024 Aug 7;2858–76.

161. Gordon IL, Stemmer EA, Wilson SE. Redistribution of blood flow after carotid endarterectomy. J Vasc Surg. 1995 Oct 1;22(4):349–60.

162. Delcanho RE, Kim YJ, Clark GT. Haemodynamic changes induced by submaximal isometric contraction in painful and non-painful human masseter using near-infra-red spectroscopy. Arch Oral Biol. 1996 June;41(6):585–96.

163. McNeil CJ, Allen MD, Olympico E, Shoemaker JK, Rice CL. Blood flow and muscle oxygenation during low, moderate, and maximal sustained isometric contractions. Am J Physiol Regul Integr Comp Physiol. 2015 Sept;309(5):R475-481.

164. Clark GT, Carter MC. Electromyographic study of human jaw-closing muscle endurance, fatigue and recovery at various isometric force levels. Arch Oral Biol. 1985 Jan 1;30(7):563–9.

165. Po E, Le T. Histochemical and morphological muscle-fibre characteristics of the human masseter, the medial pterygoid and the temporal muscles. Arch Oral Biol [Internet]. 1983 [cited 2025 July 26];28(9). Available from: https://pubmed.ncbi.nlm.nih.gov/6227313/

166. D van S, Jh DV, Ap H. Resistance of jaw-closing muscles to fatigue during repetitive maximal voluntary clenching efforts in man. Arch Oral Biol [Internet]. 1978 [cited 2025 July 26];23(8). Available from: https://pubmed.ncbi.nlm.nih.gov/281904/

167. Glagov S, Zarins C, Giddens DP, Ku DN. Hemodynamics and atherosclerosis. Insights and perspectives gained from studies of human arteries. Arch Pathol Lab Med. 1988 Oct;112(10):1018–31.

168. Raj N, Pan C, Starke AM, Matos ALL, Soehnlein O, Gerke V. Altered shear stress of blood flow causes plasma membrane damage in endothelial cells. Blood Vessels Thromb Hemost. 2025 Feb 1;2(1):100040.

169. Hensel O. Cold stimulation of the oral cavity redistributes blood towards the brain in healthy volunteers. Eur J Neurol. 2024;31(5):e16227.

170. Powell K, Lin K, Tambo W, Saavedra AP, Sciubba D, Al Abed Y, et al. Trigeminal nerve stimulation: a current state-of-the-art review. Bioelectron Med. 2023 Dec 13;9(1):30.

171. Hiebert SM, Burch E. Simulated human diving and heart rate: making the most of the diving response as a laboratory exercise. Adv Physiol Educ. 2003 Sept;27(3):130–45.

172. Yalcin ED, Aslan Ozturk EM. Ultrasonographic evaluation of the effect of splint therapy on masseter muscle and blood flow in patients with bruxism. CRANIO®. 2025 Jan 2;43(1):135–43.

173. Lavigne GJ, Khoury S, Abe S, Yamaguchi T, Raphael K. Bruxism physiology and pathology: an overview for clinicians. J Oral Rehabil. 2008;35(7):476–94.

174. Yoshimi H, Sasaguri K, Tamaki K, Sato S. Identification of the occurrence and pattern of masseter muscle activities during sleep using EMG and accelerometer systems. Head Face Med. 2009 Feb 11;5:7.

175. Reddy SV, Kumar MP, Sravanthi D, Mohsin AHB, Anuhya V. Bruxism: A Literature Review. J Int Oral Health JIOH. 2014;6(6):105–9.

176. Murali RV, Rangarajan P, Mounissamy A. Bruxism: Conceptual discussion and review. J Pharm Bioallied Sci. 2015 Apr;7(Suppl 1):S265.

177. Gibbs CH, Mahan PE, Mauderli A, Lundeen HC, Walsh EK. Limits of human bite strength. J Prosthet Dent. 1986 Aug 1;56(2):226–9.

178. Lal SJ, Sankari A, Weber DDS. Bruxism Management. In: StatPearls [Internet]. Treasure Island (FL): StatPearls Publishing; 2024 [cited 2024 Dec 12]. Available from: http://www.ncbi.nlm.nih.gov/books/NBK482466/

179. List T, Jensen RH. Temporomandibular disorders: Old ideas and new concepts. Cephalalgia. 2017 June 1;37(7):692–704.

180. Ohlmann B, Waldecker M, Leckel M, Bömicke W, Behnisch R, Rammelsberg P, et al. Correlations between Sleep Bruxism and Temporomandibular Disorders. J Clin Med. 2020 Feb 24;9(2):611.

181. Klasser GD, Greene CS. The changing field of temporomandibular disorders: what dentists need to know. J Can Dent Assoc. 2009 Feb;75(1):49–53.

182. Durham J, Newton-John TRO, Zakrzewska JM. Temporomandibular disorders. BMJ. 2015 Mar 12;350:h1154.

183. Lobbezoo F, Naeije M. Bruxism is mainly regulated centrally, not peripherally. J Oral Rehabil. 2001;28(12):1085–91.

184. Góra A, Laskowski G, Węgrzyn P, Węgrzyn K, Salińska A, Wasilewski M, et al. Diagnosis and management of bruxism. A literature review. Qual Sport. 2024 Sept 17;22:54807–54807.

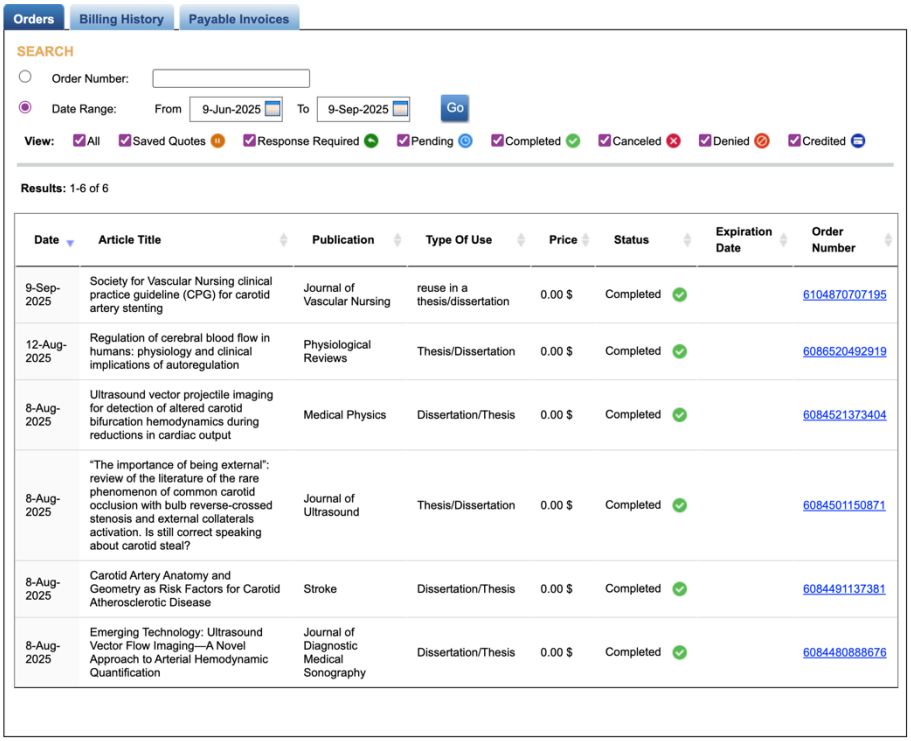
185. Thijssen DHJ, Dawson EA, Tinken TM, Cable NT, Green DJ. Retrograde flow and shear rate acutely impair endothelial function in humans. Hypertens Dallas Tex 1979. 2009 June;53(6):986–92.

186. ŞAHİN E, Baglan Uzunget S, Keskinruzgar A. Elastic Properties of the Aorta Are Affected in Young Patients with Sleep Bruxism. Int J Sci Res Dent Med Sci [Internet]. 2021 Dec [cited 2025 July 29];(Online First). Available from: https://doi.org/10.30485/ijsrdms.2021.315608.1216

187. Chiu JJ, Chien S. Effects of Disturbed Flow on Vascular Endothelium: Pathophysiological Basis and Clinical Perspectives. Physiol Rev. 2011 Jan;91(1):10.1152/physrev.00047.2009.

188. Mohammadzadeh M, Erfanian R, Khoozani AS, Abdullah H, Anari MR, Ardehali MM, et al. The Effects of Cold Application on Internal and External Carotid Artery Flows: an Evaluation of Conventional Epistaxis Management. Indian J Otolaryngol Head Neck Surg. 2025 Apr 1;77(4):1813–7.

Appendix A: Figure Permissions



Orders | Billing History | Payable Invoices

SEARCH

Order Number:

Date Range: From 9-Jun-2025 To 9-Sep-2025 Go

View: All Saved Quotes Response Required Pending Completed Canceled Denied Credited

Results: 1-6 of 6

Date	Article Title	Publication	Type Of Use	Price	Status	Expiration Date	Order Number
9-Sep-2025	Society for Vascular Nursing clinical practice guideline (CPG) for carotid artery stenting	Journal of Vascular Nursing	reuse in a thesis/dissertation	0.00 $	Completed		6104870707195
12-Aug-2025	Regulation of cerebral blood flow in humans: physiology and clinical implications of autoregulation	Physiological Reviews	Thesis/Dissertation	0.00 $	Completed		6086520492919
8-Aug-2025	Ultrasound vector projectile imaging for detection of altered carotid bifurcation hemodynamics during reductions in cardiac output	Medical Physics	Dissertation/Thesis	0.00 $	Completed		6084521373404
8-Aug-2025	"The importance of being external": review of the literature of the rare phenomenon of common carotid occlusion with bulb reverse-crossed stenosis and external collaterals activation. Is still correct speaking about carotid steal?	Journal of Ultrasound	Thesis/Dissertation	0.00 $	Completed		6084501150871
8-Aug-2025	Carotid Artery Anatomy and Geometry as Risk Factors for Carotid Atherosclerotic Disease	Stroke	Dissertation/Thesis	0.00 $	Completed		6084491137381
8-Aug-2025	Emerging Technology: Ultrasound Vector Flow Imaging—A Novel Approach to Arterial Hemodynamic Quantification	Journal of Diagnostic Medical Sonography	Dissertation/Thesis	0.00 $	Completed		6084480888676